



HAL
open science

Impact of guaiacol on the formation of undesired macromolecules during catalytic hydroconversion of bio-oil: a model compounds study

Matthieu Ozagac, Céline Bertino-Ghera, Denis Uzio, Mickael Rivallan, Dorothee Laurenti, Christophe Geantet

► To cite this version:

Matthieu Ozagac, Céline Bertino-Ghera, Denis Uzio, Mickael Rivallan, Dorothee Laurenti, et al.. Impact of guaiacol on the formation of undesired macromolecules during catalytic hydroconversion of bio-oil: a model compounds study. *Biomass and Bioenergy*, 2016, 95, pp.194-205. 10.1016/j.biombioe.2016.09.022 . hal-01487875v2

HAL Id: hal-01487875

<https://hal.science/hal-01487875v2>

Submitted on 10 Oct 2017

HAL is a multi-disciplinary open access archive for the deposit and dissemination of scientific research documents, whether they are published or not. The documents may come from teaching and research institutions in France or abroad, or from public or private research centers.

L'archive ouverte pluridisciplinaire **HAL**, est destinée au dépôt et à la diffusion de documents scientifiques de niveau recherche, publiés ou non, émanant des établissements d'enseignement et de recherche français ou étrangers, des laboratoires publics ou privés.

Impact of guaiacol on the formation of undesired macromolecules during catalytic hydroconversion of bio-oil: a model compounds study

M. Ozagac^a, C. Bertino-Ghera^{a,*}, D.Uzio^a, M. Rivallan^a, D. Laurenti^b, C. Geantet^b

^aIFP Energies Nouvelles, Rond-point de l'échangeur de Solaize, BP3, 69360 Solaize, France

^bIRCELYON, UMR5256 CNRS-UCBL, 2 avenue A. Einstein, 69626 Villeurbanne cedex, France

*Corresponding author: celine.bertino-ghera@ifpen.fr

Abstract

Although catalytic hydroconversion of pyrolysis bio-oils has been studied for many years, side reactions such as condensation or oligomerization leading to high molecular weight compounds still need comprehensive studies. In this work, the catalytic hydroconversion of D-glucose, furfural, acetic acid and guaiacol representative of pyrolysis bio-oils was investigated separately before testing a 5-component mixture. Thanks to a detailed analytical strategy (i.e. SEC, ¹³C NMR, GC, HPLC), this paper focuses on the effect of guaiacol conversion on sugar-like macromolecules. The study of single D-glucose and furfural revealed the fast production of high molecular weight compounds (up to 700 g.mol⁻¹) that were proven to further precipitate (from D-glucose). Guaiacol addition led to a decrease of the solid production through solubilizing and/or reacting with macromolecules. This phenomenon produced larger soluble macromolecules (up to 5.000 g.mol⁻¹). Results show that guaiacol and its hydroconversion products formed soluble macromolecules at **short reaction times and low temperatures**.

Keywords: biofuels; macromolecules characterization; pyrolysis bio-oil; guaiacol; D-glucose; SEC

1. Introduction

Lignocellulosic biomass is a promising feedstock that could be used as a renewable and CO₂-neutral source of energy and is expected to be an important resource for liquid transportation fuels or chemicals in a near future. Lignocellulose is commonly composed of three major fractions: 40–45 wt% of cellulose (dry composition), 25–35 wt% of hemicelluloses, 15–30 wt% of lignin and up to 10 wt% of other compounds (such as minerals) [1]. The most widely studied softwood feedstock are pine (or spruce), and cork or oak as regard to hardwoods. **Flash pyrolysis is a thermochemical process used to transform these resources into liquid** [1, 2]. However, the obtained pyrolysis bio-oils have limited end-user application due to their acidity (Total Acid Number or TAN between 70 and 120), their low heat capacity (compared to fossil fuels), their immiscibility with hydrocarbons and their thermal instability resulting from high oxygen content [3]. Oxygen is present in organic compounds but also as free water which can represent up to 30 wt% of the raw bio-oil. Since the last three decades, many laboratories have tried to perform

1 deoxygenation process inspired from petroleum feedstock catalytic hydroconversion [4].
2 However, upgrading biomass-derived oils from flash pyrolysis liquefaction to
3 hydrocarbons requires a significant oxygen removal (and consequently a high H₂
4 consumption) before any final conventional refining process.
5

6 Also called upgrading, those thermo-chemical processes deal with operational
7 temperatures up to 400°C. Nevertheless, several literature studies [4, 5] showed the
8 occurrence of fast competitive reactions such as condensation or oligomerization which
9 are prone to produce solid residues even at low temperature. This phenomenon is
10 detrimental for the process because it leads to extensive plugging of the reactor and
11 catalyst deactivation. This coking ability especially due to the bio-oils thermal instability is
12 a process limitation and needs an in-depth comprehension before any industrial scaling-
13 up. Venderbosch [5, 6] and Elliott [7] published studies describing the competition
14 between hydroconversion pathways and the production of high molecular weight
15 compounds also referred as soluble macromolecules [8 – 10]. To avoid those pathways,
16 they recommended a two-step process to firstly convert macromolecules precursor at
17 low temperatures (from 150 to 200°C) followed by a deep hydrodeoxygenation (up to
18 350°C). So far, the involved reaction mechanisms are not well described and literature is
19 largely lacking of rationalization of the chemical mechanisms.
20
21
22
23
24
25
26
27

28 The pyrolytic degradation products of lignin were generally represented by aromatic
29 **model compounds** [10 – 12] such as guaiacol, anisole or phenol derivatives. On the one
30 hand, carbohydrates, acids, ketones and furans derivatives were commonly used to
31 represent the contribution of cellulose and the hemicellulose [12, 13] fractions in the
32 flash pyrolysis liquefaction. Levoglucosan [14, 15] and D-glucose [16] are typically
33 adopted as representative compounds. Even if levoglucosan would be the model of
34 choice as it is present in high quantity in pyrolysis bio-oils, it is readily converted to D-
35 glucose in hydroconversion conditions and in **acidic water medium** [15 - 17]. On the other
36 hand, it is well established [18, 19] that hemicelluloses flash pyrolysis produces furanic
37 and carboxylic acid compounds in large amounts. **Besides well identified molecules,**
38 **heavier molecules including macromolecules are also present in the bio-oil (including**
39 **pyrolytic lignin) and those macromolecules usually precipitated by water addition. These**
40 **oligomers were characterized by typical aromatic fragments arising from lignin [10, 20].**
41 **Our purpose in this study is to investigate the macromolecules production from light**
42 **molecules during the hydroconversion reaction.**
43
44
45
46
47
48
49
50

51 Numerous studies deal with representative model molecules of bio-oils composition
52 which result from lignocellulose [11] degradation during the pyrolysis step. Because of
53 the high diversity of oxygenated compounds in a bio-oil, it is mandatory to consider at
54 least a mixture of representative compounds even if very few studies were proposed in
55 the literature. For a catalysts screening, Elliott [21] developed a three-compound mixture
56 made of guaiacol, furfural, acetic acid and water. More than thirty by-products were
57
58
59
60
61
62
63
64
65

1
2
3
4
5
6
7
8
9
10
11
12
13
14
15
16
17
18
19
20
21
22
23
24
25
26
27
28
29
30
31
32
33
34
35
36
37
38
39
40
41
42
43
44
45
46
47
48
49
50
51
52
53
54
55
56
57
58
59
60
61
62
63
64
65

quantified but no crossed-interactions between those compounds were discussed. More recently, Runnebaum [22] has studied the catalytic conversion of four compounds representing a pyrolysed lignin fraction. Nevertheless, none of those experimental studies complied with the comprehension of the high molecular compounds production.

In this paper, we have chosen D-glucose as the ex-cellulose model molecule and arising compounds from hemicellulose flash pyrolysis were represented by furfural and acetic acid. In a previous work [23] we investigated the catalytic hydroconversion of D-glucose and furfural and we observed the fast and extensive production of high molecular weight compounds even at 200°C. This trend was followed by SEC analysis and carbon balances including GC-quantified compounds. Those so called macromolecules were proven to arise from furanic and aromatic compounds that were extensively produced by D-glucose dehydration and furfural hydrolysis/hydration. In the present work, we report the catalytic hydroconversion of a mixtures constituted by D-glucose, furfural and guaiacol. Through an increase of the complexity of the mixtures and using a multi-technique characterization strategy (SEC, ¹³C NMR, GC, HPLC, etc...), this study highlights the main routes responsible for the formation of high molecular compounds and the effect of the presence of guaiacol on macromolecules.

2. Materials and Methods

2.1. Material

The D-glucose (> 99.5%), furfural (99%) and acetic acid (99%) were purchased from Sigma Aldrich and guaiacol (> 99%) from Acros Organics and n-hexadecane (99%) from Alfa Aesar. Those compounds were used as received.

To promote the hydroconversion reactions, various mono- and bi-metallic active phases were investigated. Noble metal based catalysts such as Pt, Pd or Ru exhibit high performances but remain expensive. Less performing Ni/alumina-based catalysts [24 - 26] are nevertheless an economically suitable solution for an industrial process. A proprietary NiMo/ γ -Al₂O₃ catalyst (9.2 wt% Ni, 5.4 wt% Mo) displaying hydrothermal resistance was provided by Axens. Before each reaction, fresh catalyst was crushed and sieved to particle size from 1 to 2 mm and was reduced using a hydrogen flow (0.30 m³.h⁻¹) at atmospheric pressure and 400°C during 2 h.

2.2. Experimental procedures

All catalytic reactions were carried out in an isothermal 500 cm³ stainless steel autoclave equipped with an electromagnetic driven stirrer (Rushton impeller). The methodology used and the reproducibility of the experiments are described in Supplementary Fig. S1 and S2. For each run, 150 g of feed were introduced followed by 15 g of freshly reduced catalyst transferred in a basket in an argon vessel avoiding any post-oxidation. The

1 115 reactor was hermetically closed and purged by substituting air by nitrogen and finally by
2 hydrogen. The initial pressure of hydrogen was set to 3.0 MPa before temperature
3 increase.

4
5
6 The reaction temperature ranged from 200 to 300°C. In order to limit the catalytic
7 reactions during the heating ramp (15 min to reach 250°C), the feed was vigorously
8 stirred (1,200 RPM) only once the reaction temperature was reached. This procedure was
9 120 adopted in order to limit the D-glucose conversion during the heating time. Stirring is
10 maintained during cooling down. The hydrogen addition was set to maintain a constant
11 total pressure of 13.0 MPa during the run. This procedure has been applied considering
12 the maximization of the hydrogen consumption during the catalytic hydroconversion of
13 an aqueous D-glucose (20 wt%) solution. Considering those stirring rates and catalyst
14 beads size, no external hydrodynamic limitations have been observed [23].
15
16 125

17
18
19
20
21 Once the reaction time was reached, H₂ introduction was stopped and the reactor was
22 cooled down to room temperature (10 min to cool down from 300 to 100°C). Then
23 gaseous, liquid and solid products were totally collected and separately analyzed. Gases
24 130 were collected using an auxiliary vessel and sampled in vacuum TEDLAR® bags for
25 subsequent off-line gas chromatography (GC-FID/TCD) analysis. While the reactor was
26 purged by nitrogen and unlocked, the catalytic basket was removed. The liquid phases
27 and the solid residues were separated by centrifugation at 4,000 tr.min⁻¹ during 20 min.
28
29
30
31 135 Subsequently, aqueous and organic phases were separated in a separatory funnel
32 referred respectively as "aqueous phase" and "organic phase". The recovered catalyst
33 was washed using a Thermo Scientific™ Dionex™ (ASE 150) extractor heated at 60°C and
34 under a 10 MPa acetone pressure. The catalyst and the solid residues were dried at 70°C
35 under atmospheric pressure during 12 h. Acetone was used as a washing solvent also to
36 clean the reactor and the impeller and was further removed by a vacuum rotary
37 evaporator. The obtained liquid phase will be referred as "washed phase".
38
39 140
40
41
42

43 2.3. Analytical procedures

44
45
46 145 Considering the complexity of the products, an analytical strategy was set to characterize
47 each effluent (see Supplementary Fig. S3). Each phase was analyzed separately in order to
48 determine the repartition of the carbon and to identify a maximum of compounds.
49

50
51
52 Gases were analyzed by GC (Agilent 7890A) equipped with a Flame Ionization Detector
53 (FID) and two Thermal Conductivity Detectors (TCD). Three parallel columns were used:
54 150 HP-Plot Q (30 m x 0.32 mm i.d x 20 µm), HP-Plot 5A (30 m x 0.32 mm i.d x 1 µm) and
55 PONA (50 m x 0.2 mm i.d x 0.5 µm). The carrier gas was helium. Standards were
56 periodically injected for alkanes (C1 to C6), CO, CO₂, N₂ and H₂ quantification. The oven
57 temperature program ranged from 30 to 200°C at a rate of 20°C.min⁻¹.
58
59
60
61
62
63
64
65

155 Liquid effluents were analyzed by GC (AGILENT-6890N) with a Flame Ionization Detector
1 (FID) and a RTX-35 Amine (30 m x 0.25 mm i.d x 1 μm) column. The vaporization
2 temperature was 250°C, the oven temperature program ranged from 40 to 220°C at a
3 rate of 4°C.min⁻¹. For each identified compounds, quantification was performed with 1,2-
4 propanediol as an external standard and Effective Carbon Number method (ECN) was
5 used to estimate FID response factors for oxygenates [27]. The GC/MS analysis was
6
7 160 conducted with a Thermo Trace GC/MS equipped with the same columns and program
8
9 than the GC/FID analysis. The mass analyzer is a simple quadrupole with an electron
10 ionization ion source at 70 eV. The products were identified using the NIST library.
11
12

14 The composition of the aqueous phase was also determined using a HPLC system (Waters
15 Alliance 2695), a Bio-Rad column Aminex Deashing followed by an Agilent column
16 165 Metacarb operated at 95°C. The aqueous mobile phase was set at a flow rate of 0.1
17 cm³.min⁻¹. The detector is constituted of a Differential Index Refractometer and an UV
18 detector. The analysis of a sample was complete within 100 min. The concentrations of
19 each compound (cellobiose, D-glucose, sorbitol, xylose, galactose, arabinose, mannose,
20 glycerol and xylitol) in the product mixture were determined using eight calibration
21 curves obtained by analyzing standard solutions of known concentrations.
22
23 170
24
25

27 Water content in liquid effluents was measured by a Karl Fischer (KF) Mettler Toledo V20.
28 For every sequence, a calibration procedure with a Fluka Hydranal water standard 1.0
29 was performed. Each value indicated in this study corresponds to average of three
30 175 measurements.
31
32
33

35 Soluble macromolecules contained in aqueous effluents were analyzed by non-
36 quantitative size exclusion chromatography (SEC) by a Waters system (Alliance). The
37 180 system was constituted by four columns in series (7.8 mm x 300 mm) containing 5 μm -
38 particle size with porosity ranging from 10 to 1,000 nm. During a typical analysis 50.10⁻⁶
39 m³ of sample were injected into the column. Run were performed at 30°C (columns
40 temperature) during 49 min. Two detectors were used: a refractive index-detector and a
41 UV-detector (set to three wavelengths: 214, 254 and 280 nm). Tetrahydrofuran was used
42 as mobile phase (1 cm³.min⁻¹). Standard polystyrene mixtures having various molecular
43 weights were used for calibration at the beginning of each new sequence and correspond
44 185 to a Polystyrene (PS) molecular weight ranging from 160 to 5,000 g.mol⁻¹.
45
46
47
48
49

51 In order to determine the carbon balance, a Thermo Scientific™ FLASH 2000 analyzed the
52 190 carbon deposition (CHONS) onto the catalyst and the solid residues. Grinded samples
53 were injected twice in an oven set at 950°C where CO₂ was formed. An on-line TCD
54 detector quantified this component and calculated the sample corresponding carbon
55 equivalent. Each six samples, the analyzer was controlled by a BBOT (2,5-Bis (5-tert-butyl-
56 benzoxazol-2-yl) thiophene) standard.
57
58
59

60 195

Finally, **solid phase** ¹³C MAS NMR analysis were performed on an AVANCE Bruker 400 MHz with Highpower Proton Decoupling (HPDEC) and spinning rates of 12 kHz using a CPMAS probe and 4 mm rotor. The free induction decays were obtained after excitation with 90° pulses with a repetition time of 50 s. After accumulation of 1024 scans, spectra were processed with 20 Hz Lorentzian line broadening and a 0.1 s Gaussian broadening. All ¹³C MAS NMR spectra were referenced to tetramethyl silane (TMS). Quantification of the functional groups present in each sample was determined after baseline correction by integrating over characteristic regions using TopSpin 3.0 software. Intensities over defined chemical shift windows were integrated to quantify selected C structures; 0-55 ppm (C-alkyl), 55-95 ppm (O-alkyl C including carbohydrates), 95-165 ppm (C-aromatic), 165-220 ppm (C-carbonyl in carboxylic acids, esters, amides, ketones and aldehydes).

2.4. Determination of the conversion, mass and carbon balances

As shown by the analytical strategy described previously, this study aims at understanding model compounds hydroconversion from the macroscopic scale (though experimental balance given by the Equation 1) to the molecular scale. In order to assess the accuracy of chemical pathways, carbon balances are considered taking into account each recovered phases as detailed in Equation 2. In the liquid phases, recovered carbon corresponds either to equivalent quantified carbon thought GC-FID and HPLC for the liquid phase or by Total Organic Carbon (TOC) and liquid elementary analysis (CHONS). When n-hexadecane has been used, elementary analysis of containing mixtures has not been considered.

Equation 1 : mass balance

Experimental mass loss (expressed in weight %)

$$= \frac{(m_{\text{liquid}} + m_{\text{gases}} + m_{\text{catalyst}})_{\text{introduced}} - (m_{\text{liquid}} + m_{\text{gases}} + m_{\text{catalyst}} + m_{\text{residues}})_{\text{recovered}}}{(m_{\text{liquid}} + m_{\text{gases}} + m_{\text{catalyst}})_{\text{introduced}}} \times 100$$

Equation 2 : carbon balance

Total quantified carbon (expressed in weight % of carbon equivalent)

$$= \frac{(m_{\text{C}_{\text{liquid}}})_{\text{introduced}} - (m_{\text{C}_{\text{liquid}}} + m_{\text{C}_{\text{gases}}} + m_{\text{C}_{\text{catalyst}}} + m_{\text{C}_{\text{residues}}})_{\text{recovered}}}{(m_{\text{C}_{\text{liquid}}})_{\text{introduced}}} \times 100$$

The gaseous phase is analyzed by GC-FID/TCD and the solid residues and the catalysts are assessed by a solid elementary analysis (CHNS).

1 Solving the Equation 2 implies considering the carbon contribution of each quantified
2 225 species. Hence, carbon contribution of a molecule so called "A" constituted of carbon,
3 oxygen and hydrogen atoms leads to:
4

5
6 Equation 3

7 $mC_j = wt\%C_j \cdot m_j$ and $mC_{liquid} = \sum_{i=j}^k mCi$
8
9

10 230 With:

- 11 • mC_j : mass of carbon equivalent in the compound j [g].
- 12 • $wt\%C_j$: weight carbon content of the compound j [wt%].
- 13 • m_j : mass of GC-quantified compound j [g].
- 14 • $\sum_{i=j}^k mCi$: sum of the carbon equivalents hold by the compounds "j" to "k" in the
15 liquid phase [g].
16
17 235
18
19
20

21 To consider the molecular scale, reactant (expressed as "A") conversion will be expressed
22 as:
23

24 Equation 4

25
26
$$X_i = \frac{n_{A,0} - n_A}{n_{A,0}}$$

27
28

29 240 with :

- 30 • X_A : conversion rate of "A" reactant
- 31 • $n_{A,0}$ and n_A : "A" reactant molar amount respectively at the beginning and the end
32 of the reaction [mol].
33
34
35
36
37
38

39 245 In order to compare SEC analyses with various water content liquid phases, raw signals
40 will take into account the water dilution. Thus, signals will be presented as:
41
42

43 Equation 5 :

44
$$\text{Nomalized SEC signal} = \frac{\text{Raw signal}}{100mg} \cdot \frac{1}{1 - \text{Water content}} = \frac{\text{Raw signal}}{100mg} \cdot \frac{1}{\text{Organic content}}$$

45
46

47 With:

- 48 • Raw signal / 100: Raw signal (RI or UV) normalized to a 100 mg sample [mg^{-1}].
- 49 250 • Water content: weight water content in the liquid phase [-].
- 50 • Organic content: weight organic content in the liquid phase [-].
51
52
53
54
55

56 The carbon content of solids resulting from D-glucose hydroconversion during a test "i"
57 255 containing **n-hexadecane (noted as n-C16)** onto the surface assessed by solid ^{13}C MAS
58 NMR. **Hexadecane was calibrated thanks to an external calibration (see supplementary**
59 **Figure S4). Due to the intensity of hexadecane chemical shifts, the corresponding areas**
60
61
62
63
64
65

were calculated and further subtracted to the ^{13}C NMR spectra. Thus, carbon equivalent in the solid residues were calculated following Equation 6.

Equation 6 : Carbon content in the D-glucose' residues "i" containing n-C16 assessed by solid ^{13}C MAS NMR :

$$m_{\text{cor } i} = m_{\text{raw } i} - m_{\text{n-C16}}$$

With:

- $m_{\text{cor } i}$: Corrected carbon equivalent mass of the residues for a test "i" [g].
- $m_{\text{raw } i}$: mass of carbon equivalent in the residues measured by elementary analysis for a test "i" [g].
- $m_{\text{n-C16 } i}$: Carbon equivalent mass of n-hexadecane in solid residues quantified by external calibration of the ^{13}C MAS NMR [g].

2.5. Studied mixtures

As previously described, four model molecules have been chosen for this study: D-glucose (noted as Glu) in water, furfural (noted as Fur), acetic acid (noted as AA) and guaiacol (noted as Gua).

Mixtures (see Table 1) aimed at representing well known oxygenated functions compounds but also the proportions of related families of compounds as well as pH, C-H-O atomic ratios, water content in a typical raw bio-oil [1]. Thus, guaiacol was chosen to represents the pyrolyzed lignin fraction and was introduced either at 15 or 30 wt%. D-glucose and furfural modeling respectively carbohydrate-like and their degradation compounds were introduced at 20 and 13 wt% respectively. 30 wt% of demineralized water was introduced to model free water that is contained in a typical bio-oil but also to insure the D-glucose solubility in the liquid phase at ambient conditions. Finally, 7 wt% of acetic acid was introduced to set a representative bio-oil acidity with a Total Acid Number of 120 mg potassium hydroxide introduced for one gram of mixture.

In this work, the four-compounds mixtures will be noted as "Mixture A". A second mixture in which a part of guaiacol has been replaced by n-hexadecane will be noted as "mixture B". Those mixtures comply with average bio-oil atomic ratios (dry basis) [1]. "Mixture A" H/C and O/C atomic ratios are respectively equal to 1.4 and 0.6 whereas "Mixture B" H/C and O/C atomic ratios are respectively equal to 1.8 and 0.7.

The next section is divided into three parts.

- The first part will be focused on the catalytic hydroconversion from single compounds to the final mixture "A". For both single reactants and the ternary mixtures (e.g. three-compound mixtures) hydroconversion reactions, n-

295 hexadecane has been introduced in order to complete the feed loading to 150 g.
1 For simplicity, the binary mixtures (e.g. two-compound mixtures) are reported in
2 appendix. Whatever the studied mixture, 30 wt% of demineralized water was
3 introduced. In this paragraph, chemical pathways will be discussed depending on
4 hydroconverted mixtures.
5
6

- 7 300 • In a second and third part, the effect of reaction time and temperature on the
8 Mixture A catalytic hydroconversion will be discussed. Those studies will
9 particularly emphasize the effect of guaiacol (study of Mixture “B”) on soluble
10 macromolecules production.
11
12
13
14
15

16 305 **3. Results and discussion**

17 3.1. Study of the catalytic hydroconversion leading to “Mixture A”

18
19 In these experiments, the reaction time and temperature were respectively set to 1 h and
20 250°C. These conditions can be considered as usual ones regarding to bio-oil
21 hydroconversion studies [4, 6 - 8].
22
23
24 310

25 Table 2 reports the experimental mass balances of the catalytic hydroconversion of eight
26 mixtures from the single reactant to the ternary mixtures and Mixture A. Mass balances
27 closures depend on the residue production which requires the use of a large quantity of
28 acetone as a washing solvent further evaporated in a vacuum rotary evaporator. This last
29 step has been identified as the main source of loss by evaporating lights compounds
30 dragged by the acetone. When there is no solid residues production, mass balances are
31 between 97.3 and 101.4 wt%, whereas when a large quantity of solids is produced, the
32 mass balance is between 81.3 and 88.3 wt%.
33
34
35
36
37
38
39

40 320 In the case of the conversion of single molecules, only D-glucose led to residues in a large
41 amount (8.0 g for 100 g of feed, representing 39 wt % with respect to the D-glucose
42 loading). Considering Glu/Fur/AA mixture, the solid production increased up to 14.7 for
43 100 g of feed. Nevertheless, this content was drastically reduced when guaiacol was
44 added to D-glucose and acetic acid in water (1.2 g for 100 g of feed). So, guaiacol had a
45 remarkable effect on the solid production. In comparison with the Glu/Gua/Fur mixture,
46 the catalytic hydroconversion of Mixture A also demonstrated that acetic acid promotes
47 the solids production. Indeed, 11.2 g of solids residues were produced against 0.7 g from
48 the Glu/Gua/Fur mixture.
49
50
51
52
53

54
55 To get an insight on soluble macromolecules properties, SEC-RI analyses of the aqueous
56 and organic phases from the ternary mixtures and Mixture A are reported respectively in
57 Figure 1 [A] and [B]. SEC-RI of hydroconverted single D-glucose and furfural effluents
58 were described elsewhere [23].
59
60
61
62
63
64
65

1 When D-glucose was present in the feed, soluble components ranging between 200 and
2 400 g.mol⁻¹ polystyrene equivalent (or PS eq.) were systematically observed in the
3 335 aqueous phases (Figure 1 [A]). Moreover, considering the huge amount of solid residues
4 produced during the catalytic hydroconversion of the ternary mixture D-
5 glucose/furfural/acetic acid (see Table 2), it can be hypothesized that produced
6 macromolecules were no more soluble in the aqueous phase and thus precipitated into
7 the solid phase.
8
9

10
11 340 For ternary mixtures, this property was observed as long as guaiacol was not introduced
12 in the feed. Then, the presence of guaiacol led to the formation of an organic phase.
13 Corresponding SEC-RI analyses (Figure 1 [B]) indicate the production of heavy compounds
14 up to 7,000 g.mol⁻¹ PS eq.. This may suggest that macromolecules produced from the
15 aqueous fraction (D-Glucose, Furfural) were no more precipitated into the solid phase but
16 solubilized by the organic phase in presence of guaiacol. This interesting result will be
17 345 further discussed. Without D-glucose (as shown by the Gua/Fur/AA test), it is also
18 interesting to note that resulting components arising from furfural catalytic
19 hydroconversion were mainly lower than 200 g.mol⁻¹ PS eq. in the aqueous phase.
20
21
22
23
24

25
26 350 As it has been studied in our previous work [23], D-glucose single catalytic
27 hydroconversion produces a wide range of chemicals since the chromatographic analysis
28 of liquid phase enables the identification and quantification of 46 organic compounds.
29 Main identified reactions were hydrogenolysis (production of levulinic acid or furfural),
30 hydrogenation (production of sorbitol and alcohol compounds from ketones [28]),
31 dehydration/hydration (production of 5-HMF or lactic acid) retro-aldol reaction
32 (production of propane-1,2,3-triol, propane-1,2-diol [29] and acetic acid), decarboxylation
33 355 or decarbonylation. Considering furfural single catalytic hydroconversion, we quantified
34 35 compounds involving furfural decarbonylation that produced C4 cut (furan and
35 tetrahydrofuran) and furfural hydrogenation to C5 cut (furfuryl alcohol and by-products)
36 [30 – 32]. In the same way, guaiacol catalytic hydroconversion in similar operating
37 360 conditions involved the quantification of 20 compounds GC-FID analysis. It is commonly
38 accepted [33, 34] that three main chemical pathways can be observed involving either the
39 demethylation to 1,2-benzenediol or a direct demethoxylation step to phenol. The direct
40 hydrogenation of the benzene ring is unfavored with NiMo/Alumina catalyst [35, 36].
41 Some studies [37, 38] also reported the production of heavier structures due to self-
42 365 condensation between primary products such as catechol. Nevertheless, none of them
43 has been clearly identified during this study.
44
45
46
47
48
49
50
51
52

53 Regarding the production of high molecular weight compounds reported by SEC-RI
54 analyses (Figure 1), it appeared interesting to consider the carbon balances. Thus, a global
55 carbon balance (Table 3) considering TOC and CHONS analysis respectively of the aqueous
56 370 and organic phases was evaluated for the Mixture A catalytic hydroconversion effluents
57 (experimental mass balance reported in Table 2). The initial introduced amount of carbon
58
59
60
61
62
63
64
65

1 is 58.9 g. Taking into account the experimental and the analytical errors, the carbon
2 balance for this experiment is achieved by only 1.5 wt% loss. Mixture A catalytic
3 hydroconversion led to a solid phase (as residue and coke onto the catalyst) which
4 375 contains 25.3 wt% of the initial introduced carbon. The three liquid phases represent 71.3
5 wt% of C and the gaseous phase 2.0 wt% of C (particularly through CO₂, CO and CH₄).
6

7
8 This low loss balance enabled to consider the carbon equivalent of quantified compounds
9 by HPLC-RI and GC-FID in the liquid phases (Table 4). In case of the mixture A, only 37.1
10 wt% of C have been identified by these techniques in the liquid phase compared to the
11 71.3 wt% of C identified by TOC and CHONS analysis. This balance suggests that remaining
12 380 carbon may be considered as non-quantified heavy molecular weight products solubilized
13 in the liquid phase and represented by SEC-RI analysis (Figure 1).
14
15

16
17 Thus, considering carbon balance obtained from Glu/Gua/Fur conversion, it has been
18 observed that guaiacol clearly limited the solid formation while the GC/HPLC non-
19 quantified carbon increased to 60.9 wt% (Table 4). This is consistent with the high rate of
20 soluble macromolecules detected by SEC-RI (Figure 1). On the contrary, the solid residues
21 385 (coke onto the catalyst or recovered in the reactor) obtained from Glu/Fur/AA mixture
22 contained more than 75 wt% of the initial introduced carbon.
23
24
25
26

27
28 As shown in Table 4, equivalent carbon in the gaseous phase was quantitatively negligible
29 390 in comparison with the liquid phase. Major released gaseous species (CO₂ and CO) were
30 mainly produced by D-glucose while furfural and guaiacol produced a few CH₄ (see
31 Supplementary Fig. S1).
32
33

34
35 Considering previous D-glucose, furfural and guaiacol conversion schemes, distribution of
36 GC quantified products according to reaction pathways and chemical functions in the
37 liquid effluents are reported in Supplementary data (Supplementary Fig. S3)
38 395
39

40
41 This original approach provided by a multi-scale analytical strategy demonstrated the
42 cross reaction between D-glucose and furfural leading to the production of heavy
43 molecular weight compounds. Without guaiacol in the feed those compounds are
44 precursors of solid residues [23]. To improve the system description, this study needs to
45 be completed by varying the operating conditions such as reaction time and temperature
46 400 (Supplementary Fig. S15 presents a summary scheme of parts 3.2 and 3.3).
47
48

49 3.2. Effect of the reaction time on the mixture A catalytic hydroconversion

50

51
52 In this part, the effect of the reaction time on the catalytic hydroconversion of Mixture A
53 is investigated at 250°C from t₀ (heating period of the reactor) to 180 min. Figure 2 [A]
54 405 reports the recovered amount of liquid, gas and solid effluents of each experimental test.
55
56

57
58 Before 45 min of reaction, the solid production represented less than 3 wt% of recovered
59 phases whereas the sum of the liquid phases remained stable. After 45 min, solid
60
61

1 deposition onto the reactor and the catalyst increased to reach 15.1 g at 3 h. This trend
2 was heightened at 180 min while no liquid organic phase has been recovered (orange
3 410 square dots on Figure 2 [A]). Experimental losses were systematically inferior to 10 wt%.
4 Complete experimental balances as well as hydrogen consumptions are available in
5 Supplementary data (Supplementary Table S2 and Fig. S7).
6

7
8 The carbon balance illustrated in Figure 2 [B] was obtained considering the HPLC-RI and
9 GC-FID quantified carbon in the liquid phases (sum quantification from the three liquid
10 415 phases). It indicates that the worst quantification in the liquid phases was reached at 45
11 min. Above 60 min of reaction, the solid production increased as well as the
12 quantification in the liquid phases. In addition, the gas production (mainly composed by
13 CO, CO₂ and CH₄) represented only from 0.4 to 2.3 wt% of C.
14
15
16
17

18 The evolution of the main chemical functions and reactions observed for the products of
19 420 catalytic hydroconversion of mixture A, according to the residence time, are reported in
20 Supplementary data (Supplementary Fig. S8). It can be noted that at the early stages of
21 the reaction, dehydration is the predominant reaction. Those reactions were likely arising
22 from D-glucose conversion [23] even during the heating time (t₀). During this period,
23 carbonyls (including furanic species) and carboxylic acids (such as levulinic acid or lactic
24 425 acid) were widely produced. Thus, GC analyzed compounds in the liquid phases were
25 mainly composed by carbonyls and acids progressively converted into alcohols and
26 hydrocarbons. This evolution is consistent with the H₂ consumption and appeared to arise
27 between 45 and 60 min of reaction (Supplementary Table S2).
28
29
30
31
32
33

34 Nevertheless, considering the carbon balances (Figure 2 [B]), the GC and HPLC
35 430 quantification represents only a fraction of the organic compounds produced. An
36 additional representation of the evolution of the liquid phases is given by normalized SEC-
37 RI (see Figure 3) and SEC-UV 254 nm (Supplementary Fig. S9) elugrams.
38
39
40

41 Heavy compounds reached their maximum intensity within 15 min concomitantly with D-
42 glucose and furfural conversion. As previously observed [23], D-glucose was totally
43 435 converted after the heating period (t₀) contributing to the production of heavy molecular
44 weight compounds. Furfural, totally converted within 45 min, is also responsible for this
45 production. As reported in Figure 3 [B], products were likely soluble in the organic phases
46 until 45 min of reaction since a few solid residues were observed. With the increase of the
47 reaction time, the recovered organic phases decreased (See Figure 2 [A]) and completely
48 disappeared at 180 min of reaction time. In the aqueous phase (Figure 3 [A]), two intense
49 440 peaks were detected: a 248 g.mol⁻¹ PS eq. peak was ascribed to an unidentified D-glucose
50 conversion product and a 160 g.mol⁻¹ PS eq. peak belonging to 1,2-benzenediol. The
51 evolution of the latter peak is linked to the recovered guaiacol mass (quantified by GC-
52 FID) as illustrated by Figure 4. In the feed, 45 g of guaiacol was introduced.
53
54
55
56
57
58
59
60
61
62
63
64
65

445 Figure 4 also reports the ratio between GC-quantified guaiacol products carbon
1 equivalent and carbon equivalent released from guaiacol conversion. GC-quantifiable
2 guaiacol products were 1,2-benzenediol and phenol. At the very beginning of the
3 reaction, less than 1 % of introduced guaiacol was converted. Nevertheless, only 11.7 wt%
4 of the released carbon was actually quantified by GC-FID. Further, more than 45 % of
5 guaiacol was converted but less than 1 wt% of the released carbon was actually ascribed
6 to it GC-quantifiable products. Finally, from 45 min, guaiacol conversion significantly
7 450 decreased (as shown by a higher GC-FID quantification of this compound in Figure 4) and
8 a growth of its products was observed.
9

10
11
12
13
14 Three chemical pathways might describe guaiacol behavior during the catalytic
15 hydroconversion:
16 455

- 17 - Firstly, guaiacol can be converted into GC-quantifiable hydroconversion products
18 (such as phenol or 1,2-benzenediol). If so, the sum of carbon equivalent of those
19 products would be necessarily equal to the sum of carbon equivalent from the
20 guaiacol conversion.
21
- 22 460 - Guaiacol or its products can react with heavy molecular weight compounds
23 product precursors issued from D-glucose and furfural (for example in Figure 4
24 through the formation of a hemi-acetal by nucleophilic addition followed by
25 dehydration). For a high guaiacol conversion rate, only few products will be
26 quantified by GC. In this case, the sum of carbon equivalent of GC-quantifiable
27 products is away from the sum of carbon equivalent from the guaiacol conversion.
28 465
- 29 - At last, guaiacol could be not affected by the hydroconversion conditions and
30 remains in the organic phase. In this last case, a low guaiacol conversion rate as
31 well as low by-products detection would be observed.
32
33
34
35
36
37

38 Referring to Figure 4, until 45 min of reaction, guaiacol quantification reached 19.4 g (i.e.
39 56 % of conversion) while less than 0.3 wt% of C of its products were quantified by GC-
40 470 FID. This yield suggests that guaiacol or its conversion products readily reacted with D-
41 glucose and furfural macromolecule precursors [23] to produce heavier structures still
42 soluble in the organic phase. Regarding the experimental balances (Figure 2 [A]), this
43 pathway seems to prevent the solid residues production observed when increasing the
44 amount of soluble macromolecule in the organic phase (Figure 3 [B]). Indeed, between 45
45 475 min and 60 min, recovered guaiacol mass increased while the yields of GC-quantifiable
46 products slightly increased. This trend suggests that soluble heavy molecular weight
47 compounds initially formed with guaiacol were further converted by hydrogenolysis.
48 Then, beyond 45 min of reaction, residual macromolecules were no longer soluble in the
49 organic phase and precipitated resulting in the decrease of intensities of SEC-RI signal
50 480 (Figure 3 [B]).
51
52
53
54
55
56
57

58 In order to confirm the guaiacol role, a *Mixture B* (see feed compositions in Table 1) has
59 been converted under similar operating conditions. This mixture, in which 15 % of
60
61
62
63
64
65

1
2 485 guaiacol were replaced by n-hexadecane, produced 50 wt% solid more than Mixture A. As
3 previously studied [23], those structures were observed from D-glucose hydroconversion
4 suggesting chemical pathway involving furanic species (i.e. 5-HMF, furfural, etc.)
5 production subsequently converted into macromolecules precursors. From Mixture B
6 hydroconversion, liquid phase analysis revealed that a higher amount of dehydration
7 reactions occurred. Those reactions were identified to promote the production of
8 macromolecules.
9 490

10
11 Solid residues were highly made of carbon (up to 70 wt% of C). Reported ¹³C NMR in
12 Supplementary data (Supplementary Fig. S10), confirms that Mixture B solids residues
13 were containing less aromatics and alkyl compounds and more carbonyl functions.
14 Considering the high content of oxygen in the solid residues (25 wt% on average) and
15 their ¹³C NMR analysis, the precipitation suggests a change of the organic phase, like for
16 instance a decrease of the polarity during the hydroconversion for long reaction time.
17 495 Atomic carbon ratios did not change significantly with reaction time.
18
19
20
21

22
23 As an intermediate conclusion, these results highlight the fast conversion of D-glucose
24 and furfural leading to macromolecules precursors. It has been observed that guaiacol
25 500 and its products led to the formation of larger soluble macromolecules until 45 min of
26 reaction. Afterwards, the GC analysis revealed the recovery of guaiacol and its product
27 (1,2-benzenediol) simultaneously with the precipitation of macromolecules.
28
29
30

31 3.3. Effect of temperature on the mixture A catalytic hydroconversion

32
33 To improve the understanding of *Mixture A* catalytic hydroconversion, the effect of
34 505 temperature was investigated. Thus, studied temperature were 200, 250 and 300°C.
35 Complete experimental balances as well as hydrogen consumptions are reported in
36 Supplementary data (Supplementary Table S3 and Fig. S11). Figure 5 [A] and [B] displays
37 respectively the experimental and carbon balances of those three experiments.
38
39
40

41
42 At the lowest temperature, the liquid phases were mainly obtained (about 85 wt%),
43 510 containing most of the initially introduced carbon (i.e. 58.9 g verified by CHONS
44 elementary analysis). Nevertheless, as indicated in Figure 5 [B], carbon content quantified
45 by GC in the liquid phases was low. Temperature appears to strongly affect the effluent
46 distribution by producing a larger amount of solid residues and gas from 250°C (Figure 5
47 [A]). From the GC-FID analysis, reported in Supplementary data (Supplementary Fig. S12),
48 we can observe that higher temperature led to an increase of the alcohols function
49 515 production mostly from hydrogenolysis reaction. This will be further discussed
50 considering the guaiacol conversion.
51
52
53
54

55
56 From a global point of view, SEC-RI analysis (Figure 6) and carbon balances (Figure 5 [B])
57 revealed that soluble macromolecules formed the main part of the products.
58
59
60
61
62
63
64
65

520 Those SEC-RI analyses (SEC-UV 254 nm reported in supplementary Fig. S13) also indicated
1 the chemical pathways modifications between 250 and 300°C involving the
2 the disappearance of a 248 g.mol⁻¹ PS eq. peak (supposed from D-glucose products)
3 subsequently replaced by a 160 g.mol⁻¹ PS eq. peak (ascribed to 1,2-benzenediol). Those
4 two peaks were already observed during the previous reaction time. This behavior
5
6
7 525 modification is confirmed regarding the recovered guaiacol mass and guaiacol products
8 quantified by GC reported in Table 5.
9

10
11 As previously discussed, while the same quantity of guaiacol was recovered, its role was
12 completely dependent on the temperature. At 200°C, only 0.4 wt% of the carbon
13 equivalent from guaiacol conversion was quantified. This suggests that **it** reacted with D-
14 glucose and furfural macromolecules precursors. This result may explain the absence of
15 530 solid residues in the resulting effluent. Further, 250°C seems to be the breaking point
16 favoring the production of solid residues but still for a low amount of guaiacol
17 hydroconversion products. Finally, at 300°C, guaiacol was converted up to 17 wt% of C of
18 the carbon equivalent into aromatic products (as 1,2-benzenediol). Then, the **guaiacol**
19 conversion **limited the** macromolecules solubilization and **promoted** the solid formation.
20 Furthermore, decarbonylation and decarboxylation reactions increased between 250 and
21 300°C (Supplementary Fig. S12). This may lead to the production of less polar high
22 molecular weight compounds in the liquid phase which were less prone to react with
23 535 guaiacol (and its product) and precipitated.
24
25
26
27
28
29
30

31 540 To get an insight of produced solids at 250 and 300°C, ¹³C NMR analysis were performed
32 (Supplementary Fig. S14). The ¹³C NMR spectra obtained for the two residues confirm the
33 previous observations. Indeed, although solid residues contain mostly aromatic and
34 aliphatic functional groups, temperature clearly affects the structures. Then, aromatic
35 groups dropped from 65 % carbon atoms at 250°C to 57 % carbon atoms at 300°C
36 suggesting that guaiacol (or its products as 1,2-benzenediol) was slightly less involved in
37 the soluble macromolecules formation at higher temperatures. The decrease of the
38 polarity of the solid precursors is in agreement with the elementary analysis of solids
39 545 containing 40.5 and 33.5 wt% of oxygen respectively at 250 and 300°C as previously
40 suggested in the case of coal derived liquids [39].
41
42
43
44
45
46

47 550 Following the previous studies, the temperature is also a key parameter for this process.
48 In every case, D-glucose and furfural were proven to be very reactive compounds mainly
49 leading to macromolecules precursors. In order to limit the solid production, the mixture
50 should be processed at low temperature to initially promote the reaction of guaiacol with
51 macromolecules precursors. In this way, those structures are stabilized in the organic
52 phase.
53
54
55

56 **4. Conclusions**

57
58
59
60
61
62
63
64
65

1 Furfural and D-glucose catalytic hydroconversion led to a wide range of soluble
2 macromolecules or precursors that were prone to precipitate in a water medium.
3 Guaiacol addition limits the solid formation and lead to larger macromolecules (up to
4 560 5,000 g.mol⁻¹) soluble in the organic phase. This phenomenon was mainly observed at low
5 temperature and short reaction time suggesting that guaiacol was not converted into its
6 light usual hydroconversion products. At high temperature or long reaction time guaiacol
7 was mainly converted into light aromatic compounds and contributed in a lesser extent to
8 the macromolecule solubilization. This was observed simultaneously with the production
9 of solid residues.
10
11 565

12
13
14 The control of the macromolecules and subsequent solid production remains the main
15 drawback of the industrial bio-oil hydroconversion process. Moreover, in order to go
16 further and to better control the contact time and the temperature before reaction, a
17 similar study could be done in continuous reactor including an on-line sampling system.
18
19 570 In the same operating conditions and thanks to the developed analytical strategy (i.e. SEC,
20 ¹³C NMR, GC, HPLC), the effect of the presence of guaiacol during the bio-oil
21 hydroconversion was studied and will be the topic of a following paper.
22
23
24

25 **5. Appendix**

26
27
28 Supplementary data associated with this article can be found, in the online version.
29

30 575 **6. Acknowledgments**

31
32 Authors thanks for fruitful discussions and reviews of this paper: F. Albrieux, N. Charon, A.
33 Le Masle and V. Souchon from IFPEN. In addition, M. Ozagac is grateful to F. Neyret-
34 Martinez, R. Comte and S. Sivault.
35
36

37 **7. References**

- 38
39
40 580 [1] A. V. Bridgwater, Review of fast pyrolysis of biomass and product upgrading, Biomass
41 Bioener. 38 (2012) 68-94
42
43
44 [2] E. Furimsky, Catalytic hydrodeoxygenation, Appl. Catal., A. 199 (2000) 147-190
45
46
47 585 [3] A. Oasmaa and P. Peacocke, A guide to physical property characterisation of biomass-
48 derived fast pyrolysis liquids, VTT Publications 731 (2010) Espoo
49
50
51 [4] D. C. Elliott, Historical developments in hydroprocessing bio-oils, Energ. Fuel. 21 (2007)
52 1792-1815
53
54
55 590 [5] R. H. Venderbosch, H. J. Heeres, Pyrolysis oil stabilisation by catalytic hydrotreatment,
56 in: Biofuel's engineering process technology, Dr. Marco Aurelio Dos Santos Bernardes
57 (Ed.), (2011) 385-410, Rijeka
58
59
60
61
62
63
64
65

- 1 595 [6] R. H. Venderbosch, A. R., Ardiyanti, J. Wildschut, A. Oasmaa, H. J. Heeres, Stabilization
2 of biomass-derived pyrolysis oils, *J. Chem. Tech. Biotechnol.* 85 (2010) 674-686
3
4
5
6 [7] D. C. Elliott, S. J. Lee, T. R. Hart, Stabilization of Fast Pyrolysis Oil: Post Processing,
7 PNNL report – 21549 (2012) Washington
8
9 600
10 [8] E. Hoekstra, S. R. A. Kersten, A. Tudos, D. Meier, K. J. A. Hogendoorn, Possibilities and
11 pitfalls in analyzing (upgraded) pyrolysis oil by size exclusion chromatography (SEC), *J.*
12 *Anal. Appl. Pyrol.* 91 (2011) 76-88
13
14
15
16 605 [9] M. Castellví Barnés, J. P. Lange, G. van Rossum, S. R. A. Kersten, A new approach for
17 bio-oil characterization based on gel permeation chromatography preparative
18 fractionation, *J. Anal. Appl. Pyrol.* 113 (2015) 444-453
19
20
21
22 [10] R. Bayerbach, V. D. Nguyen, U. Schurr, D. Meier, Characterization of the water-
23 insoluble fraction from fast pyrolysis liquids (pyrolytic lignin): Part III. Molar mass
24 610 characteristics by SEC, MALDI-TOF-MS, LDI-TOF-MS, and Py-FIMS, *J. Anal. Appl. Pyrol.* 77
25 (2006) 95-101
26
27
28
29 [11] T. A. Milne, F. Agblevor, M. Davis, S. Deutch, D. Johnson, Development in thermal
30 biomass conversion, Blackie Academic and Professional (1997) London
31 615
32
33
34 [12] J. H. Marsman, J. Wildschut, F. Mahfud, H. J. Heeres, Identification of components in
35 fast pyrolysis oil and upgraded products by comprehensive two-dimensional gas
36 chromatography and flame ionisation detection, *J. Chrom.* 1150 (2007) 21-27
37
38 620
39
40 [13] H. Yang, R. Yan, H. Chen, D. H. Lee, C. Zheng, Characteristics of hemicellulose,
41 cellulose and lignin pyrolysis, *Fuel* 86 (2007) 1781–1788
42
43
44 [14] R. Gunawan, X. Li, A. Larcher, X. Hu, D. Mourant, W. Chaiwat, H. Wu, C. Zhu Li,
45 625 Hydrolysis and glycosidation of sugars during the esterification of fast pyrolysis bio-oil,
46 *Fuel* 95 (2012) 146-151
47
48
49
50 [15] A. B. Bindwal, P. D. Vaidya, Kinetics of aqueous-phase hydrogenation of levoglucosan
51 over Ru/C catalyst, *Ind. Eng. Chem. Res* 52 (2013) 17781-17789
52
53 630
54
55 [16] T. P. Vispute, G. W. Huber, Production of hydrogen, alkanes and polyols by aqueous
56 phase processing of wood-derived pyrolysis oils, *Green Chem.* 11 (2009) 1433-1445
57
58
59
60
61
62
63
64
65

1 [17] S. Helle, N. M. Bennett, K. Lau, J. H. Matsuib, S. J. B. Duffb, A kinetic model for
2 635 production of glucose by hydrolysis of levoglucosan and cellobiosan from pyrolysis oil,
3 Carbohydr. Res. 342 (2007) 2365–2370
4

5 [18] R. Mariscal, P. Maireles-Torres, M. Ojeda, I. Sádaba, M. López Granados, Furfural: a
6 renewable and versatile platform molecule for the synthesis of chemicals and fuels,
7 640 Energ. Environ. Sci. 9 (2016) 1144-1189
8
9

10 [19] F.-X. Collard and J. Blin A review on pyrolysis of biomass constituents: Mechanisms
11 and composition of the products obtained from the conversion of cellulose,
12 hemicelluloses and lignin, Renew. Sustain. Energ. Rev. 38 (2014) 594-608
13
14
15

16 645 [20] R. Bayerbach, D. Meier, Characterization of the water-insoluble fraction from fast
17 pyrolysis liquids (pyrolytic lignin). Part IV: Structure elucidation of oligomeric molecules, J.
18 Anal. Appl. Pyrolysis 85 (2009) 98–107
19
20
21

22 [21] D. C. Elliott, T. R. Hart, Catalytic hydroprocessing of chemical models for bio-oil,
23 650 Energ. Fuel 23 (2009) 631-637
24
25
26

27 [22] R. C. Runnebaum, T. Nimmanwudipong, D. E. Block, B. C. Gates, Catalytic conversion
28 of compounds representative of lignin-derived bio-oils: a reaction network for Guaiacol,
29 anisole, 4-methylanisole, and cyclohexanone conversion catalysed by Pt/[gamma]-Al₂O₃,
30 655 Catal. Sci. Technol. 2 (2012) 113-118
31
32
33
34

35 [23] M. Ozagac, C. Bertino-Ghera, D. Uzio, M. Rivallan, D. Laurenti, C. Geantet, Biomass
36 Bioener. (2016) (Submitted)
37
38

39 660 [24] C. Boscagli, K. Raffelt, T. A. Zevaco, W. Olbrich, T. N. Otto, J. Sauer, J.-D. Grunwaldt,
40 Mild hydrotreatment of the light fraction of fast-pyrolysis oil produced from straw over
41 nickel-based catalysts, Biomass Bioener. 83 (2015) 525–538
42
43
44

45 [25] A. R. Ardiyanti, S. A. Khromova, R. H. Venderbosch, V. A. Yakovlev, I. V. Meliín-
46 665 Cabrera, H. J. Heeres, Catalytic hydrotreatment of fast pyrolysis oil using bimetallic Ni–Cu
47 catalysts on various supports, Appl. Catal., A. 449 (2012) 121-130
48
49
50

51 [26] A. R. Ardiyanti, M. V. Bykova, S. A. Khromova, W. Yin, R. H. Venderbosch, V. A.
52 670 Yakovlev, H. J. Heeres, Ni-Based Catalysts for the Hydrotreatment of Fast Pyrolysis Oil,
53 Energ. Fuel 30 (2016) 1544-1554
54
55
56
57
58
59
60
61
62
63
64
65

1 [27] J. T. Scanlon and D. E. Willis, Calculation of flame ionization detector relative
2 response factors using the effective carbon number concept, *J. Chromatogr. Sci.* 23 (1985)
3 675 333-340
4

5 [28] J. Wildschut, J. Arentz, C. B. Rasrendra, R. H. Venderbosch, H. J. Heeres, Catalytic
6 hydrotreatment of fast pyrolysis oil: Model studies on reaction pathways for the
7 carbohydrate fraction, *Environ. Progr. Sustain. Energ.* 28 (2009) 450-460
8
9

10 680 [29] L. Vilcocq, A. Cabiac, C. Especel, E. Guillon, D. Duprez, Transformation of sorbitol to
11 biofuels by heterogeneous catalysis: chemical and industrial considerations, *Oil Gas Sci.*
12 *Tech.* 68 (2013) 841-860
13
14
15

16 [30] S. Sitthisa, T. Pham, T. Prasomsri, T. Sooknoi, R. G. Mallinson, D. E. Resasco,
17 Conversion of furfural and 2-methylpentanal on Pd/SiO₂ and Pd-Cu/SiO₂ catalysts, *J. Catal.*
18 685 280 (2011), 17-27
19
20
21

22 [31] S. Sitthisa, D. E. Resasco, Hydrodeoxygenation of furfural over supported metal
23 catalysts: a comparative study of Cu, Pd and Ni, *Catal. Lett.* 141 (2011), 784-791
24 690
25
26

27 [32] S. Sitthisa, T. Sooknoi, Y. Ma, P. B. Balbuena, D. E. Resasco, Kinetics and mechanism
28 of hydrogenation of furfural on Cu/SiO₂ catalysts, *J. Catal.* 277 (2011) 1-13
29
30
31

32 695 [33] E. Laurent, B. Delmon, Study of the hydrodeoxygenation of carbonyl, catalytic and
33 guaiacyl groups over sulfided CoMo/Al₂O₃ and NiMo/Al₂O₃ catalysts: I. Catalytic reaction
34 schemes, *Appl. Catal., A.* 109 (1994) 77-96
35
36
37

38 [34] E. Laurent, B. Delmon, Study of the hydrodeoxygenation of carbonyl, carboxylic and
39 guaiacyl groups over sulfided CoMo/Al₂O₃ and NiMo/Al₂O₃ catalyst: II. Influence of water,
40 700 ammonia and hydrogen sulfide, *Appl. Catal., A.* 109 (1994) 97-115
41
42
43

44 [35] V. N. Bui, D. Laurenti, P. Afanasiev, C. Geantet, Hydrodeoxygenation of guaiacol with
45 CoMo catalysts. Part I: Promoting effect of cobalt on HDO selectivity and activity, *Appl.*
46 *Catal. B Environ.* 101 (2011) 239-245
47 705
48
49

50 [36] V. N. Bui, D. Laurenti, P. Delichère, C. Geantet, Hydrodeoxygenation of guaiacol: Part
51 II: support effect for CoMoS catalysts on HDO activity and selectivity, *Appl. Catal. B*
52 *Environ.* 101 (2011) 246-255
53
54

55 710 [37] S. Li, S. Zhang, F. Feng, Y. Yan, Coke formation in the catalytic cracking of bio-oil
56 model compounds, *Environ. Progr. Sustain. Energ.* 34 (2015) 240-247
57
58
59
60
61
62
63
64
65

1 [38] M. V. Bykova, O. A. Bulavchenko, D. Yu Ermakov, M. Yu Lebedev, V. A. Yakovlev, V. N.
2 715 Parmon, Guaiacol hydrodeoxygenation in the presence of Ni-containing catalysts, Catal.
3 Ind. 3 (2011) 15-22
4

5 [39] J. Stihle, D. Uzio, C. Lorentz, N. Charon, J. Ponthus, C. Geantet, Detailed
6 characterization of coal-derived liquids from direct coal liquefaction on supported
7 catalysts, Fuel 95 (2012) 79-87
8 720
9

	Single reactants			Ternary mixtures				Four-compound mixtures	
	Gua	Fur	Glu	Glu/Fur/AA	Glu/Gua/AA	Gua/Fur/AA	Glu/Gua/Fur	Mixture A	Mixture B
Water	30	30	30	30	30	30	30	30	30
D-Glucose	0	0	20	20	20	0	20	20	20
Furfural	0	13	0	13	0	13	13	13	13
Acetic acid	0	0	0	7	7	7	0	7	7
Guaiacol	30	0	0	0	30	30	30	30	15
n-C16	40	57	50	30	13	20	7	0	15

Table 1 : Composition in wt% of the single, three and four-compound (ternary) mixtures

		Single reactants			Ternary mixtures				Mixture A
		Gua	Fur	Glu	Glu/Fur /AA	Glu/Gua /AA	Gua/Fur /AA	Glu/Gua/ Fur	
Inlet	Liquid phase (g)	150	150	150	150	150	150	150	150
	Reduced catalyst (g)	14.1	14.3	14.5	14.2	14.1	14.2	14.1	14.3
	Introduced H ₂ (g)	2.3	3.6	2.5	2.7	2.1	3.2	2.9	2.2
Outlet	Liquid phase (g)	151.9	142.9	105.7	85.9	140.4	149.4	139.3	108.8
	Gaseous phase without H ₂ (g)	0	0.8	2.7	3.1	2.9	0.2	3.1	4.1
	Solid residues (g)	0	0	11.9	22.1	1.8	1.3	0.7	11.2
	Catalyst (g)	14.9	15.7	18.5	22.3	15.3	15	15.9	21
	Experimental loss (wt%)	-1.4	3.9	15.7	18.7	2.5	-0.2	3.7	11.7
	H ₂ consumption /introduced	0.2	0.5	0.2	0.1	0.1	0.4	0.4	0.1
H ₂ consumption /introduced reactant (mol/mol)	0.5	4.1	1.3	0.4	0.2	0.8	0.7	0.1	

Table 2 : Mass balances of single reactants, ternary mixtures and Mixture A
(Gua/Fur/AA/Glu) hydroconversion at 250°C during 1 h

	Feed	Recovered fractions						Carbon Balance Loss
	Mixture A	Liquid organic phase	Liquid aqueous phase	Washed liquid phase	Gas phase	Catalyst	Solid residues	
Weight of equivalent carbon (g)	58.9	2.2	4.9	34.9	1.2	7.0	7.8	- 0.9
Percentage of recovered equivalent carbon (wt %)	-	3.7	8.3	59.3	2.0	12.0	13.3	- 1.5

Table 3 : Global carbon balance of Mixture A (Gua/Fur/AA/Glu) catalytic hydroconversion at 250°C during 1 h

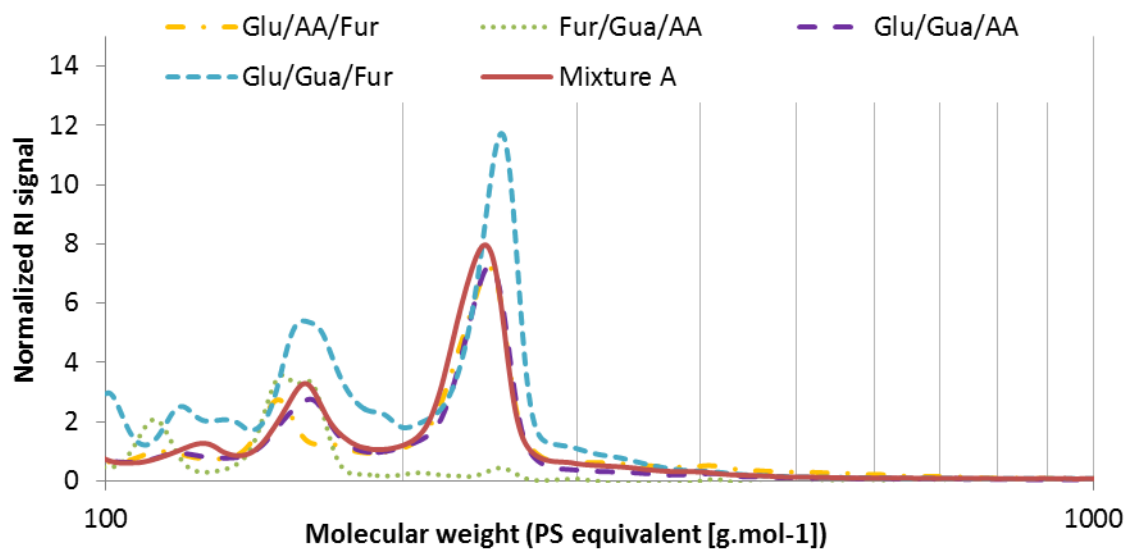
	Single reactants			Ternary mixtures				Mixture A
	Gua	Fur	Glu	Glu/Fur/AA	Glu/Gua/AA	Gua/Fur/AA	Glu/Gua/F	
Inlet (gC)	30.5	12.5	12.0	28.4	46.7	46.9	54.7	58.9
Liquid phases (wt%)	83.1	38.2	5.9	13,7	70.0	64.3	35.5	37.1
Gaseous phase (wt%)	0.0	1.8	6.5	3,9	1.9	0.3	1.8	2.0
Catalyst (wt%)	0.0	5.8	15.5	11,7	1.5	0.6	1.8	12.0
Solid residues (wt%)	0.0	0.0	44.6	65,1	0.0	0.0	0.0	13.3
Not quantified (wt%)	16.9	54.2	27.5	5,5	26.6	34.7	60.9	35.8

Table 4 : Carbon balances of single reactants, ternary mixtures and Mixture A

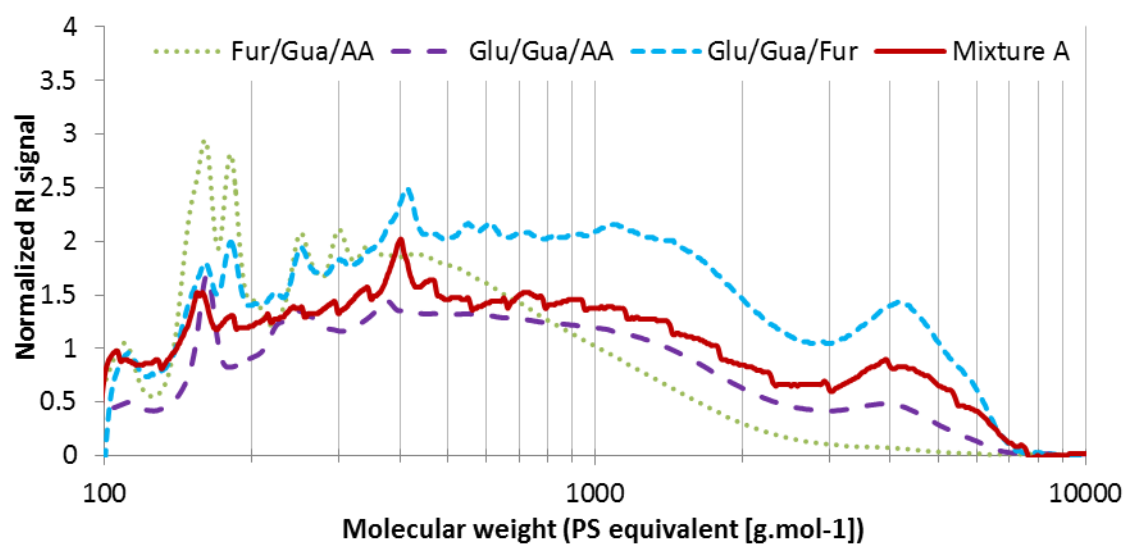
(Gua/Fur/AA/Glu) catalytic hydroconversion at 250°C during 1 h

	200°C	250°C	300°C
Quantified guaiacol (g)	27.2	27.3	29.0
GC quantified guaiacol products carbon / converted (wt%)	0.4	1.1	16.7

Table 5 : Guaiacol recovered mass and GC-quantified products yields as function of temperature (1 h)



[A]



[B]

Figure 1 : Normalized SEC-RI analysis of ternary mixtures and mixture A (Gua/Fur/AA/Glu) catalytic hydroconversion: [A] Aqueous phases, [B] Organic phases

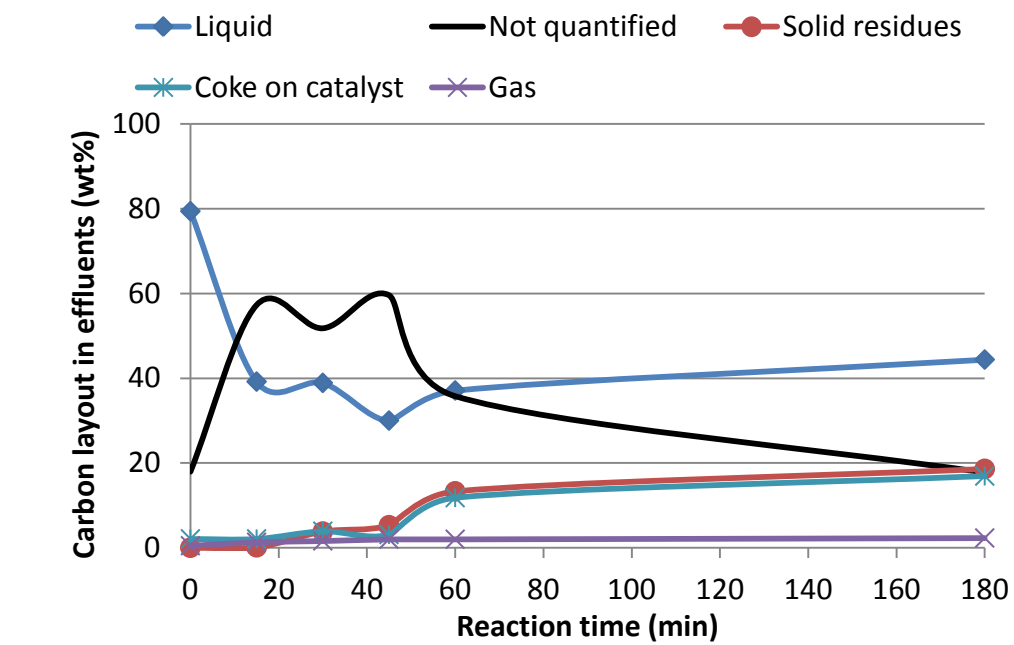
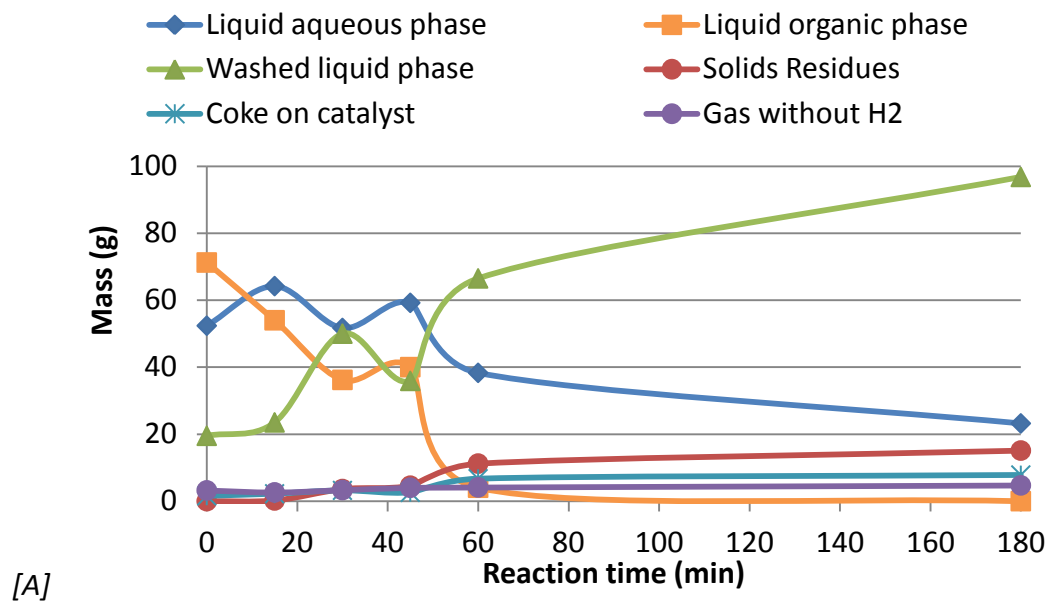


Figure 2 : [A] Experimental mass and [B] carbon balances of Mixture A (Gua/Fur/AA/Glu) hydroconversion as function of time (250 °C)

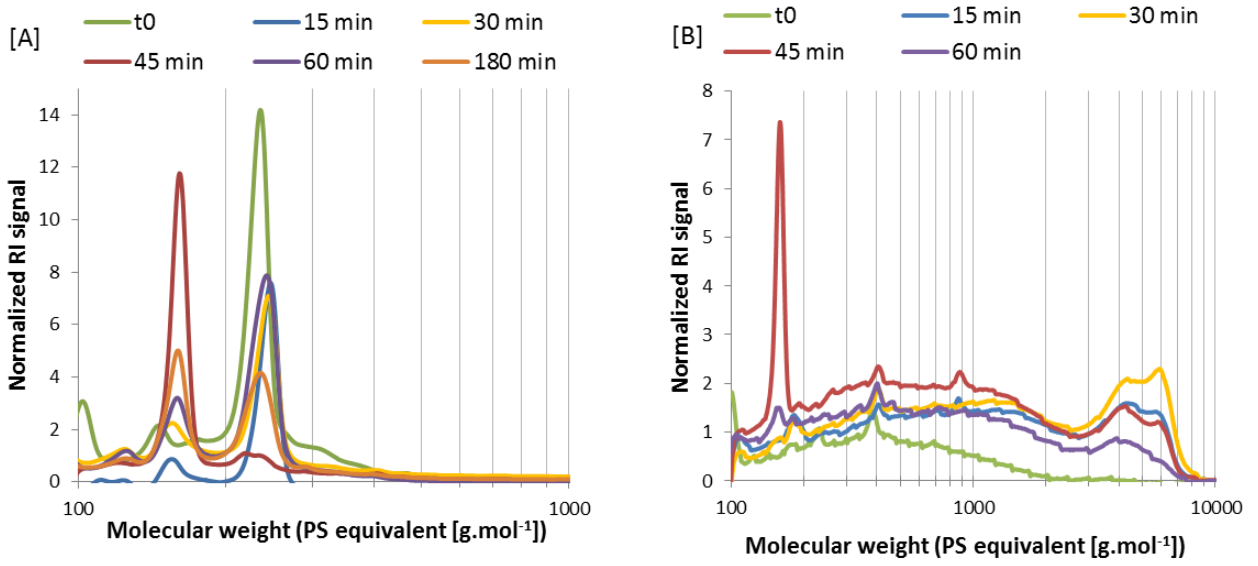


Figure 3 : Normalized SEC-RI analyses of Mixture A (Gua/Fur/AA/Glu) hydroconversion as a function of time (250 °C): [A] Aqueous phases, [B] Organic phases

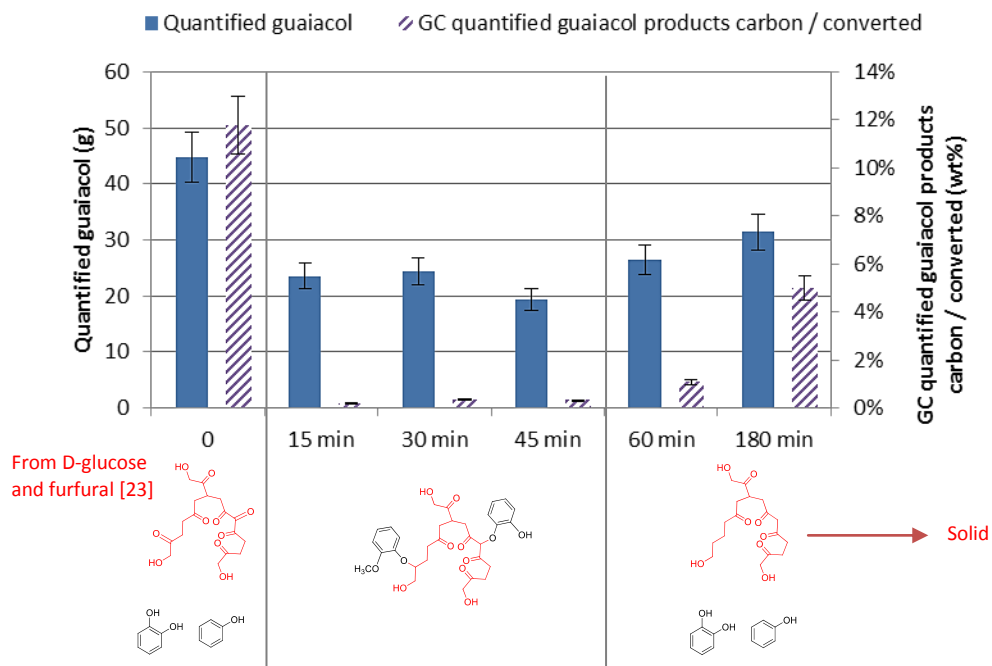


Figure 4 : Recovered guaiacol weight (left axis) and GC-quantified products carbon equivalent (right axis) as a function of time (250 °C)

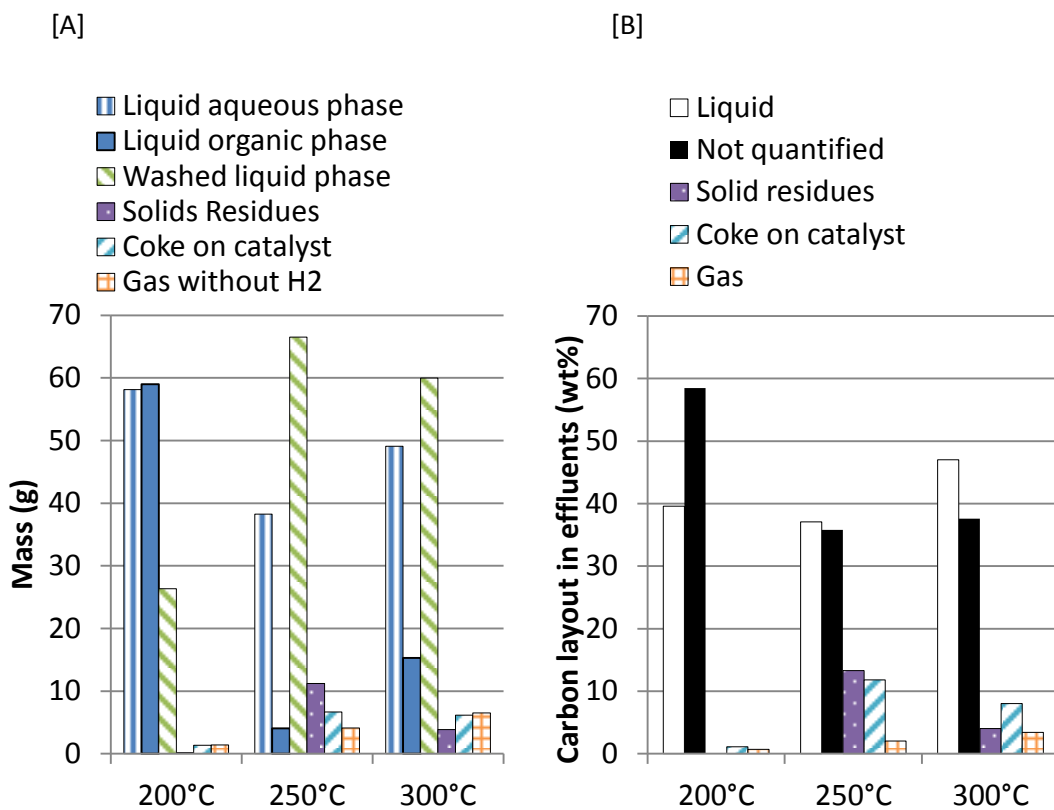


Figure 5 : [A] Experimental mass and [B] carbon balances of Mixture A (Gua/Fur/AA/Glu) hydroconversion as function of temperature (1 h)

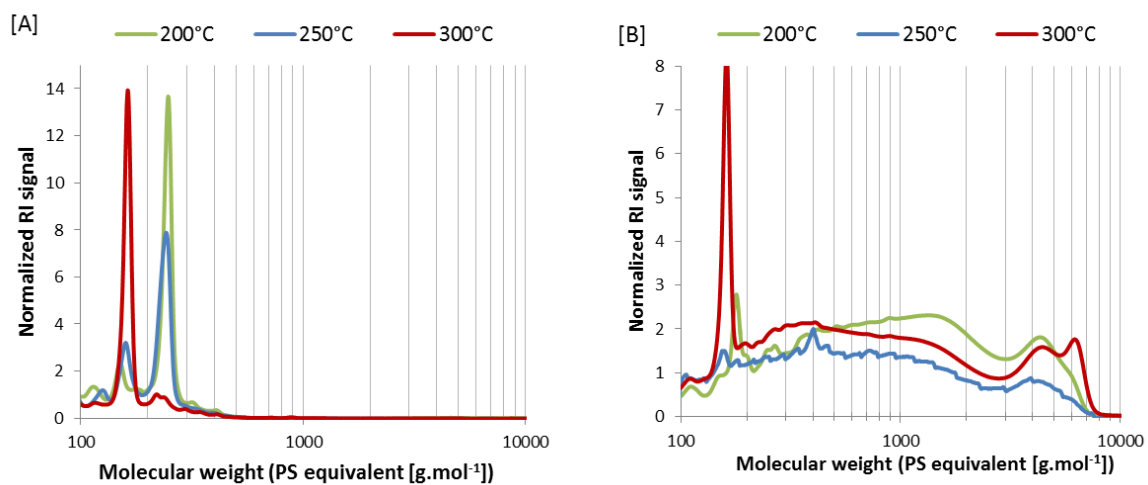


Figure 6 : Normalized SEC-RI analysis of mixture A (Gua/Fur/AA/Glu) catalytic hydroconversion as function of temperature (1 h): [A] Aqueous phases, [B] Organic phases

Impact of guaiacol on the formation of undesired macromolecules during catalytic hydroconversion of bio-oil: a model compounds study

M. Ozagac^a, C. Bertino-Ghera^{a,*}, D.Uzio^a, M. Rivallan^a, D. Laurenti^b, C. Geantet^b

^a*IFP Energies Nouvelles, Rond-point de l'échangeur de Solaize, BP3, 69360 Solaize, France*

^b*IRCELYON, UMR5256 CNRS-UCBL, 2 avenue A. Einstein, 69626 Villeurbanne cedex, France*

**Corresponding author: celine.bertino-ghera@ifpen.fr*

Supplementary

2. Materials and Methods

2.2. Experimental procedures

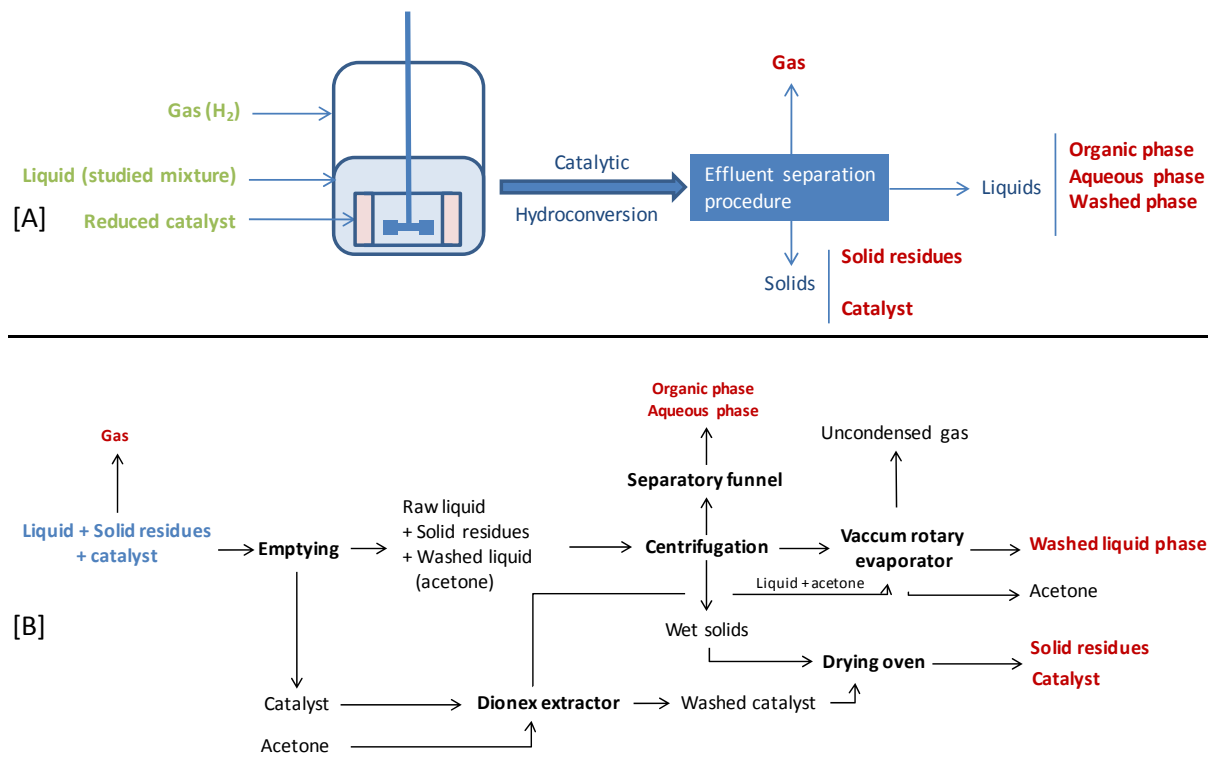


Figure S1 : Schematized experimental procedure [A] global [B] detailed

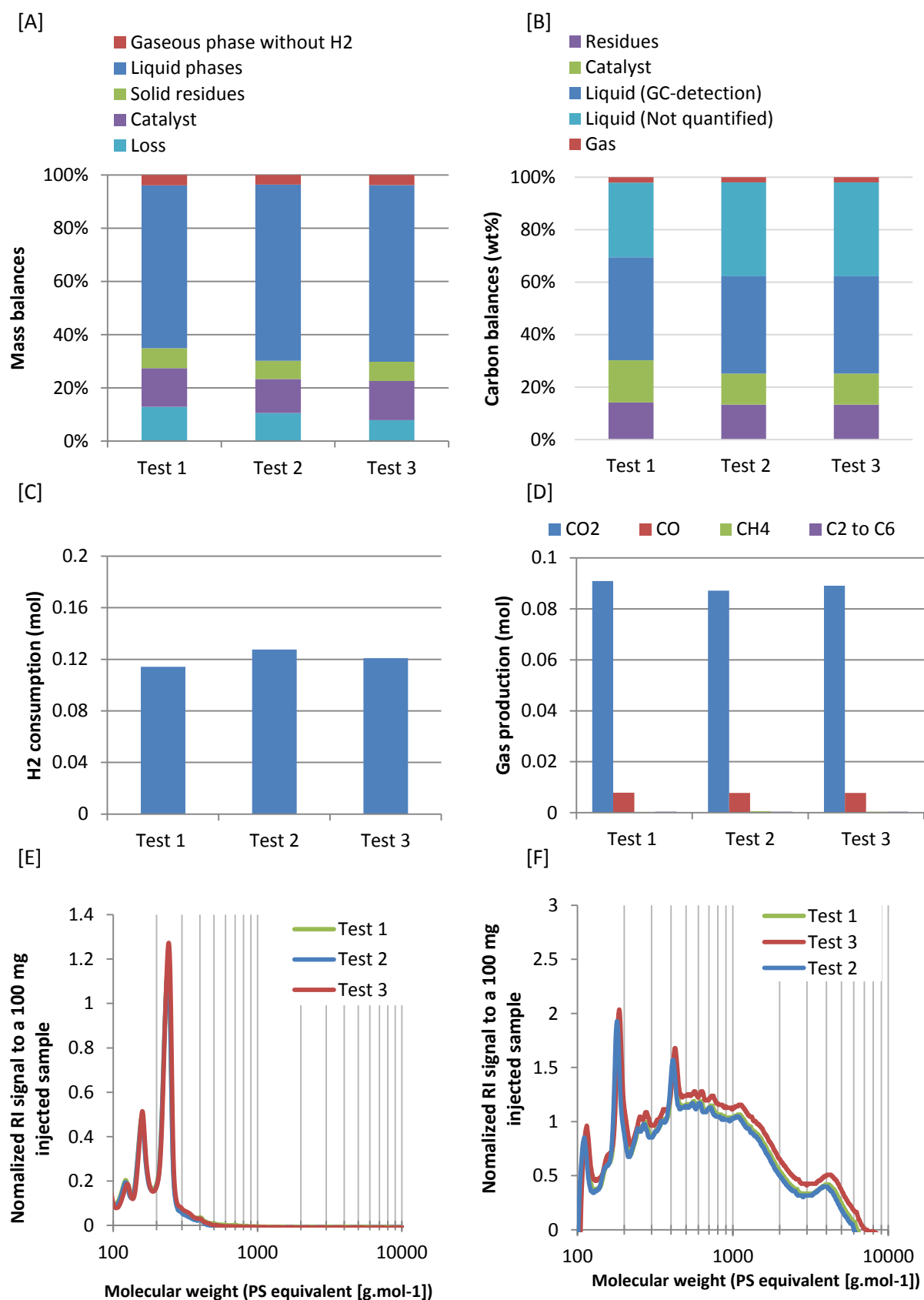


Figure S2 : Repeatability tests of the 5-compound mixture catalytic hydroconversion at 250°C during 1 h. [A] Mass balances, [B] Carbon balances from GC quantification of the liquid phases, [C] Hydrogen consumption, [D] Gas production, [E] SEC-RI analysis of the aqueous phases, [F] SEC-RI analysis of the organic phases

2.3. Analytical procedures

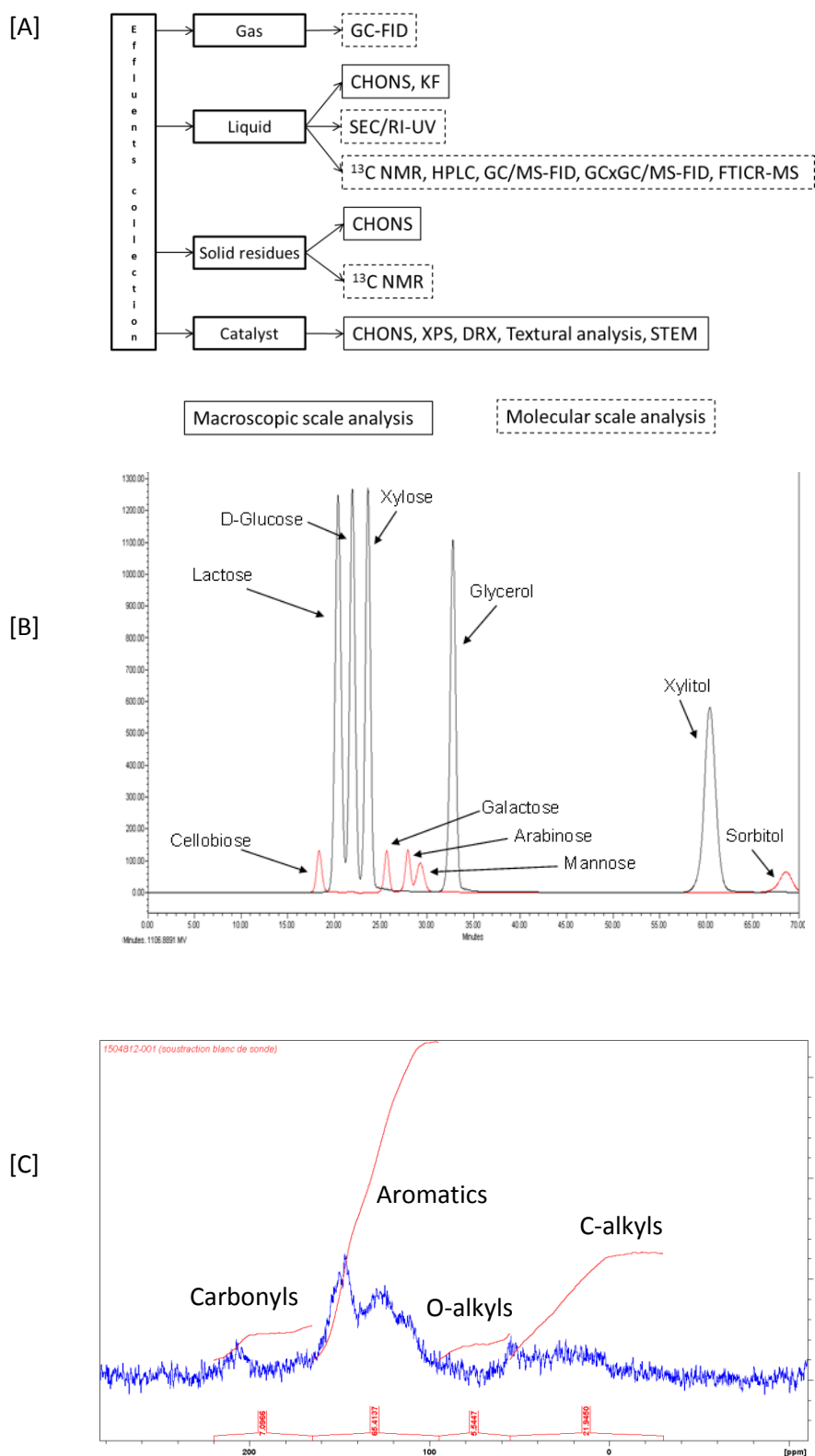


Figure S3 : [A] General analytic procedure, [B] HPLC-RI calibration, [C] Example of a ¹³C NMR spectra of the solid residue produced from D-glucose at 250°C, 3 h

3. Results and discussion

3.1. Study of the catalytic hydroconversion leading to "Mixture A"

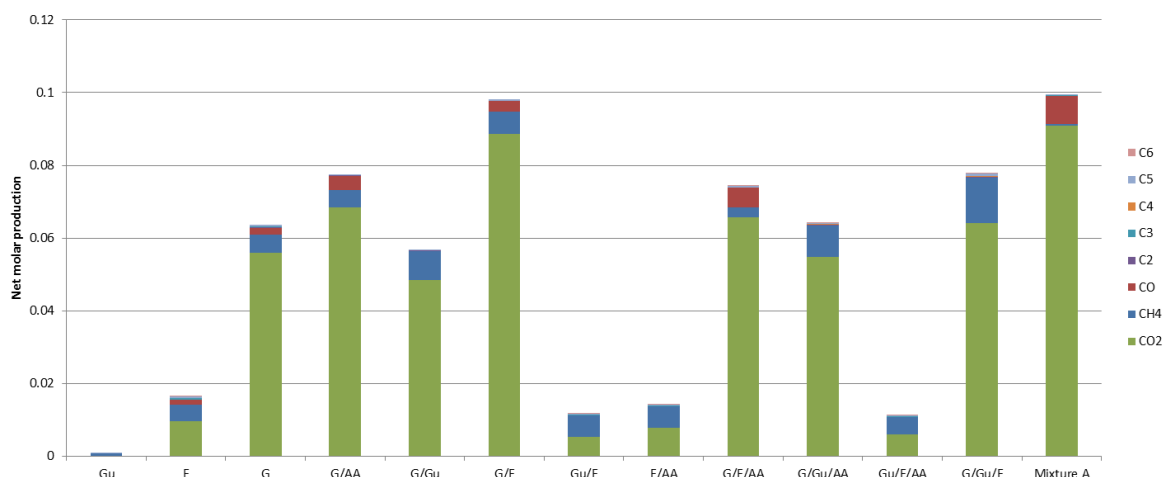
Table S1 reports the mass balances of the two-compound mixtures hydroconversion (250°C – 1 h).

		Binary mixtures				
		G/AA	G/Gu	G/F	Gu/F	F/AA
Inlet	Liquid phase (g)	150	150	150	150	150
	Water (wt%)	30	30	30	30	30
	D-Glucose (wt%)	20	20	20	0	0
	Furfural (wt%)	0	0	13	13	13
	Acetic acid (wt%)	7	0	0	0	7
	Guaiacol (wt%)	0	30	0	30	0
	n-C16 (wt%)	43	20	37	27	50
	Reduced catalyst (g)	14.4	14.5	14.2	14.1	14.1
	Introduced H ₂ (g)	2.3	2.7	2.5	3.6	3.3
Outlet	Liquid phase (g)	121.6	140.1	80.5	143.7	129.1
	Gaseous phase without H ₂ (g)	3.2	2.3	4.4	0.4	0.5
	Solid phase (g)	5.2	0.4	14.3	0.5	1.3
	Catalyst (g)	15.3	15.6	24.9	15.0	15.4
	Experimental loss (wt%)	11.6	4.0	24.3	3.7	11.4
	H ₂ consumption/introduced	0.1	0.2	0.2	0.5	0.4
	H ₂ consumption / introduced reactant (mol/mol)	0.4	0.6	0.6	1.5	1.8

Index : G (D-glucose), Gu (Guaiacol), F (Furfural), AA (Acetic Acid)

Table S1 : Experimental balances of the two-compounds mixtures hydroconversion (250°C – 1 h)

Gaseous phases analysis from mixtures hydroconversion are reported in Figure S4.



Index : G (D-glucose), Gu (Guaiacol), F (Furfural), AA (Acetic Acid)

Figure S4 : Net molar production in the gas phases from single to mixture A catalytic hydroconversion (250°C – 1 h)

Figure S5 illustrates the reaction scheme for guaiacol catalytic hydroconversion in the operating conditions. 20 compounds were detected by GC-FID analysis of recovered liquid phase.

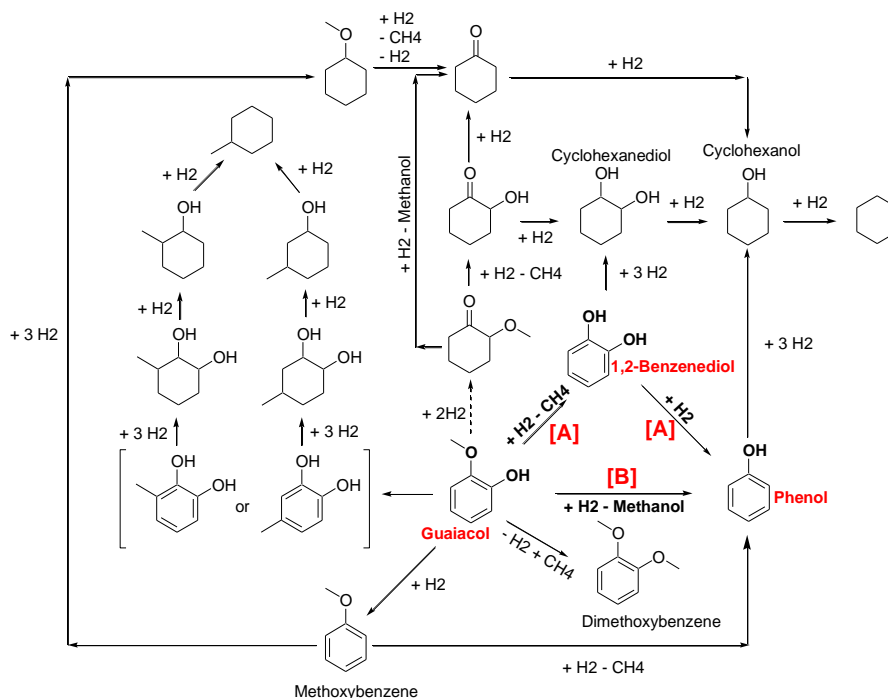


Figure S5: Guaiacol catalytic hydroconversion reaction pathways from GC-FID analysis

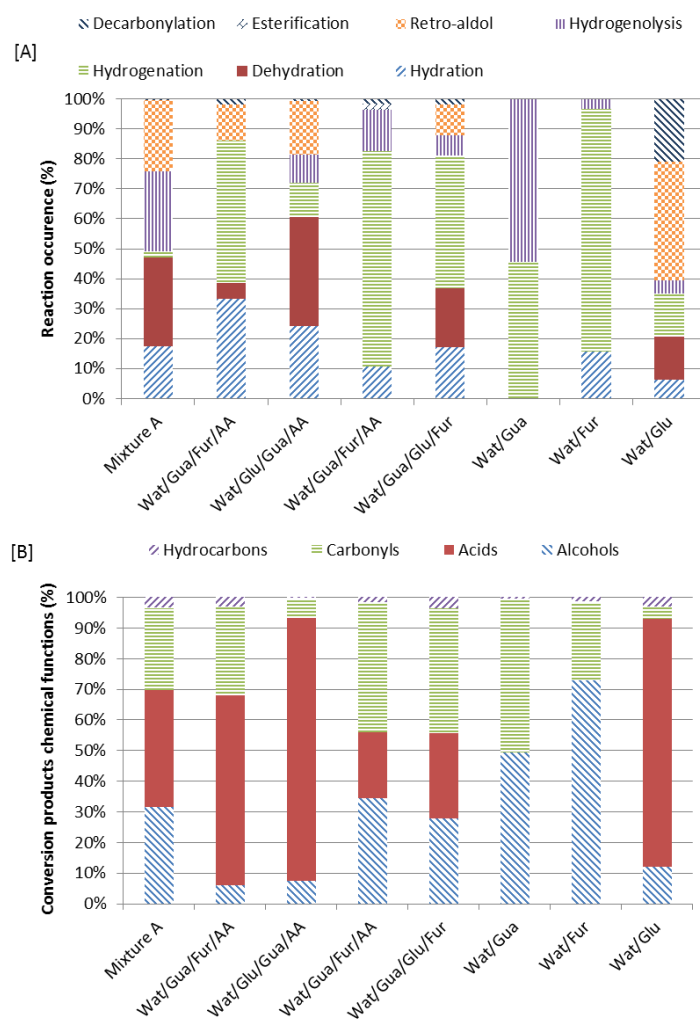


Figure S6 : Mixture A, ternary mixture and single quantified products (250°C – 1 h) [A] Chemical reaction distribution, [B] Chemical functions distribution from Mixture A

Considering previous reaction schemes [23] and Figure S5, distribution of GC detected products according to reaction pathways and chemical functions in the liquid effluents are reported respectively in Figure S6 [A] and [B]. These representations aim at evidencing the main reactions trends observed during the catalytic hydroconversion of *Mixture A*. For Figure S6 [A] simplification, when two pathways were identified to produce the same product, only the main one was considered. For example, 1,2-benzenediol is assumed to be produced only from guaiacol hydrogenolysis and the D-glucose pathway was omitted. For Figure S6 [B], each compound with two oxygenated functions has been accounted twice. The furfural and D-glucose conversion were 100 % for all the experiments. Acetic acid is considered as a reactant but also a D-glucose by-product, therefore no conversion is considered. Those products were quantified by GC and HPLC.

Mixture A conversion products appeared to arise from various chemical pathways producing equally carbonyls, acids and alcohols species. As previously shown, those distributions were

similar to the ternary system Glu/Gua/Fur. Guaiacol involved an increase of hydrogenation reactions (Figure S6 [A]) which is in line with H₂ consumptions reported in Table S1. D-glucose hydroconversion mainly resulted from water-equilibrated reactions (hydration/dehydration/retro-aldol). The presence of acetic acid did not seem to affect much the organic function distributions of GC-FID detected compounds.

3.2. Effect of the reaction time on the mixture A catalytic hydroconversion

Table S2 reports the mass balances.

Reaction time (min)		0	15	30	45	60	180
Inlet	Liquid phase (g)	150	150	150	150	150	150
	Reduced catalyst (g)	14.49	14.1	14	13.9	14.3	14.2
	Introduced H ₂ (g)	2.56	1.8	2.2	2.2	2.2	2.5
Outlet	Global liquid phases (g)	143.1	141.7	138	135.1	108.8	120
	• Liquid aqueous phase (g)	52.4	64.2	51.7	59.2	38.3	23.2
	• Liquid organic phase (g)	71.2	54	36.2	40	4	0
	• Washed liquid phase (g)	19.5	23.5	50	35.9	66.5	96.8
	Gaseous phase without H ₂ (g)	3.2	2.6	3.3	4	4.1	4.7
	Solids (g)	0	0.2	3.6	4.6	11.2	15.1
	Catalyst (g)	16.1	16.3	17.2	16.5	21	22
	Experimental loss (wt%)	2.7	2.0	1.3	2.4	11.7	1.8
	H ₂ consumption/introduced	0.12	0.11	0.13	0.15	0.12	0.34
	H ₂ consumption / introduced reactant (mol/mol)	0.17	0.14	0.16	0.18	0.14	0.26

Table S2 : Experimental balances of Mixture A hydroconversion as function of time (250 °C)

Figure S7 reports the gas production arising from Mixture A hydroconversion as a function of time.

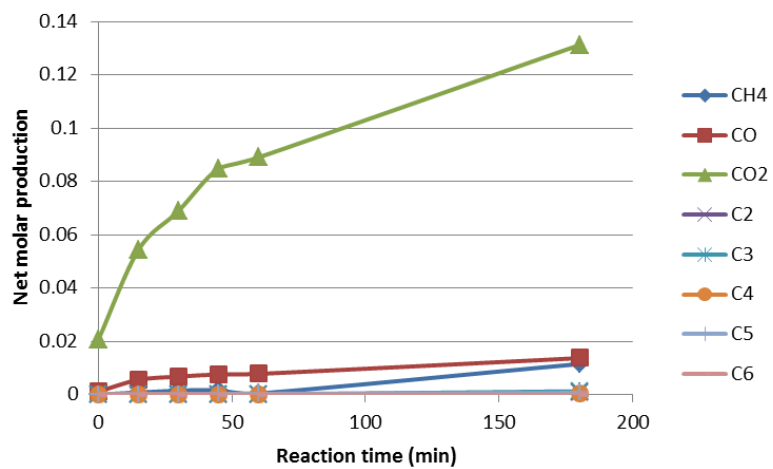


Figure S7 : Net molar production from mixture A catalytic hydroconversion (250°C)

The evolution of the main chemical functions and reactions observed for the products of catalytic hydroconversion of mixture A, according to the residence time, are reported in Figure S8.

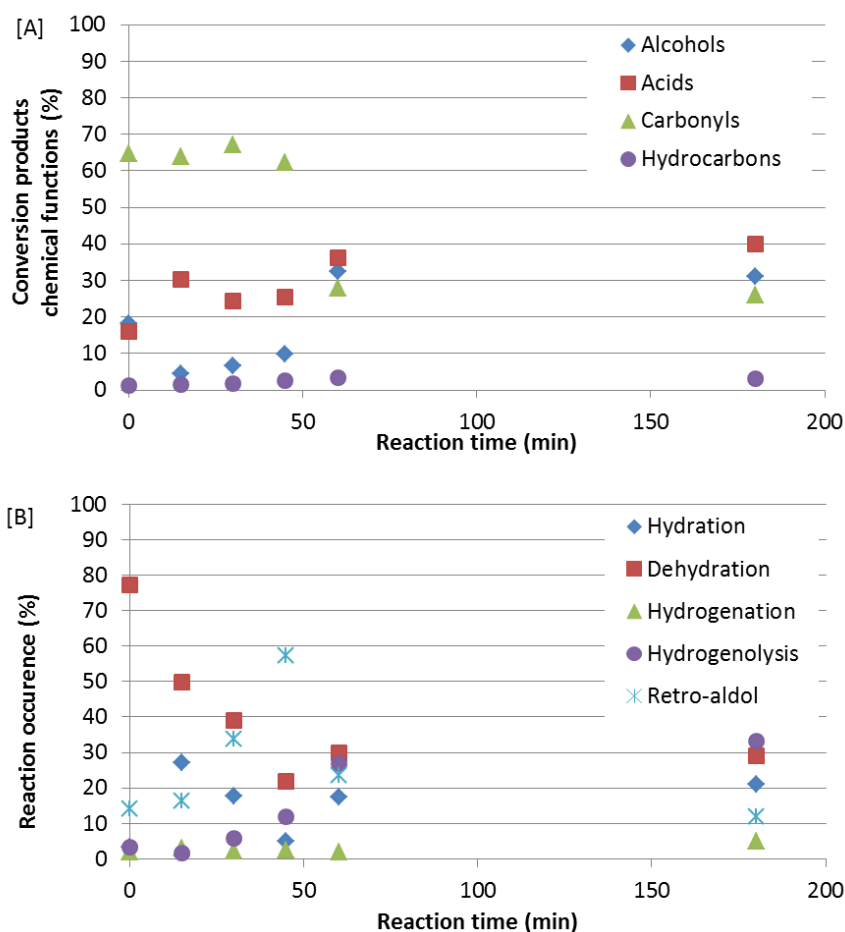


Figure S8 : Mixture A from quantified products as a function of time (250 °C) [A] Chemical functions distribution, [B] Chemical reactions distribution

It can be noted that at the early stages of the reaction, dehydration is the predominant reaction. Those reactions were likely arising from D-glucose conversion [22] even during the heating time (t_0). During this period, carbonyls (including furanic species) and carboxylic acids (such as levulinic acid or lactic acid) were widely produced. As illustrated in Figure S8 [B], retro-aldol reactions and hydrogenolysis reactions leading to shorter deoxygenated molecules species only appears predominantly from 45 min. This suggests some reaction pathways modifications confirmed by Figure S8 [A] between 45 min and 60 min. Thus, GC analyzed compounds in the liquid phases were mainly composed by carbonyls and acids progressively converted into alcohols and hydrocarbons. This evolution is consistent with the H_2 consumption and appeared to arise between 45 and 60 min of reaction (see Table S2).

Figure S9 reports the normalized SEC-UV254 nm analyses of liquid phases from Mixture A as a function of time.

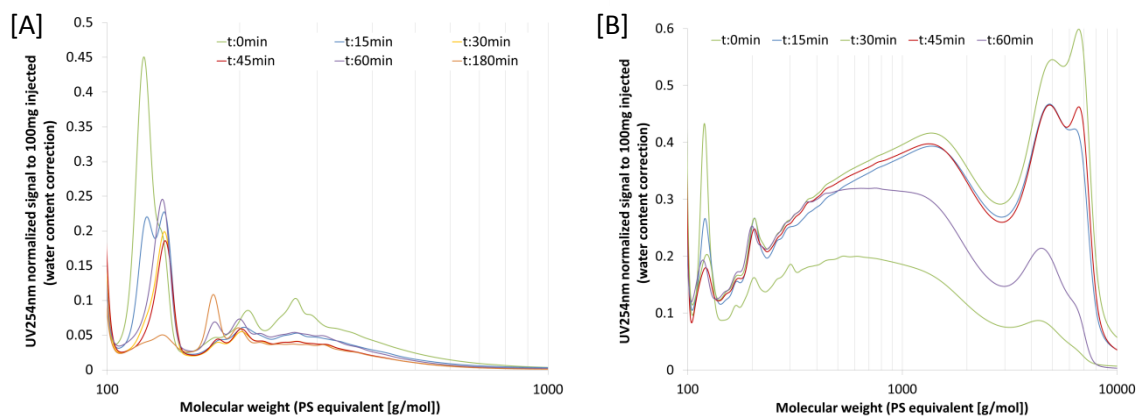


Figure S9 : Normalized SEC-UV254 nm analyses of Mixture A hydroconversion as a function of time: [A] Aqueous and [B] Organic phases (250°C)

Solid from mixtures A and B were analyzed by ^{13}C NMR. Distribution are reported in Figure S10.

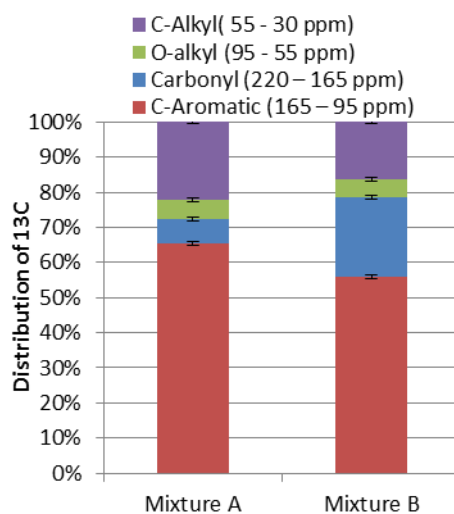


Figure S10 : ^{13}C NMR of Mixture A and B catalytic hydroconversion solid residues (250°C, 1 h)

3.3. Effect of temperature on the mixture A catalytic hydroconversion

Table S3 reports the mass balances.

Reaction temperature (°C)		200°C	250°C	300°C
Inlet	Liquid phase (g)	150.0	150.0	150.0
	Reduced catalyst (g)	14.3	14.3	14.4
	Introduced H ₂ (g)	3.5	2.2	1.4
Outlet	Global liquid phases (g)	143.4	108.8	124.4
	• Liquid aqueous phase (g)	58.1	38.3	49.1
	• Liquid organic phase (g)	59.0	4.0	15.3
	• Washed liquid phase (g)	26.3	66.5	60.0
	Gaseous phase without H ₂ (g)	1.4	4.1	6.5
	Solids (g)	0.2	11.2	3.8
	Catalyst (g)	15.6	21.0	20.6
	Experimental loss (wt%)	2.7	11.7	5.8
	H ₂ consumption/introduced (mol/mol)	0.3	0.1	0.3
	H ₂ consumption / introduced reactant (mol/mol)	0.5	0.1	0.3

Table S3 : Experimental balances of Mixture A hydroconversion as function of reaction temperature (1 h)

Figure S11 reports the gas production arising from Mixture A hydroconversion as a function of the temperature.

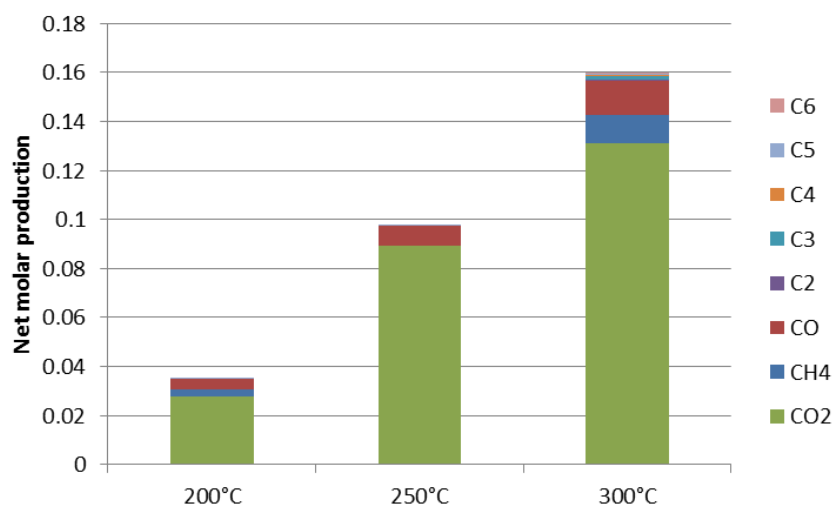


Figure S11: Net molar production from mixture A catalytic hydroconversion (1 h)

Liquid phases were analyzed by GC-FID and HPLC. Figure S12 reports the Chemical functions distribution and the chemical reaction distribution. We can observe that higher temperature led to an increase of the alcohols function production mostly from hydrogenolysis occurred.

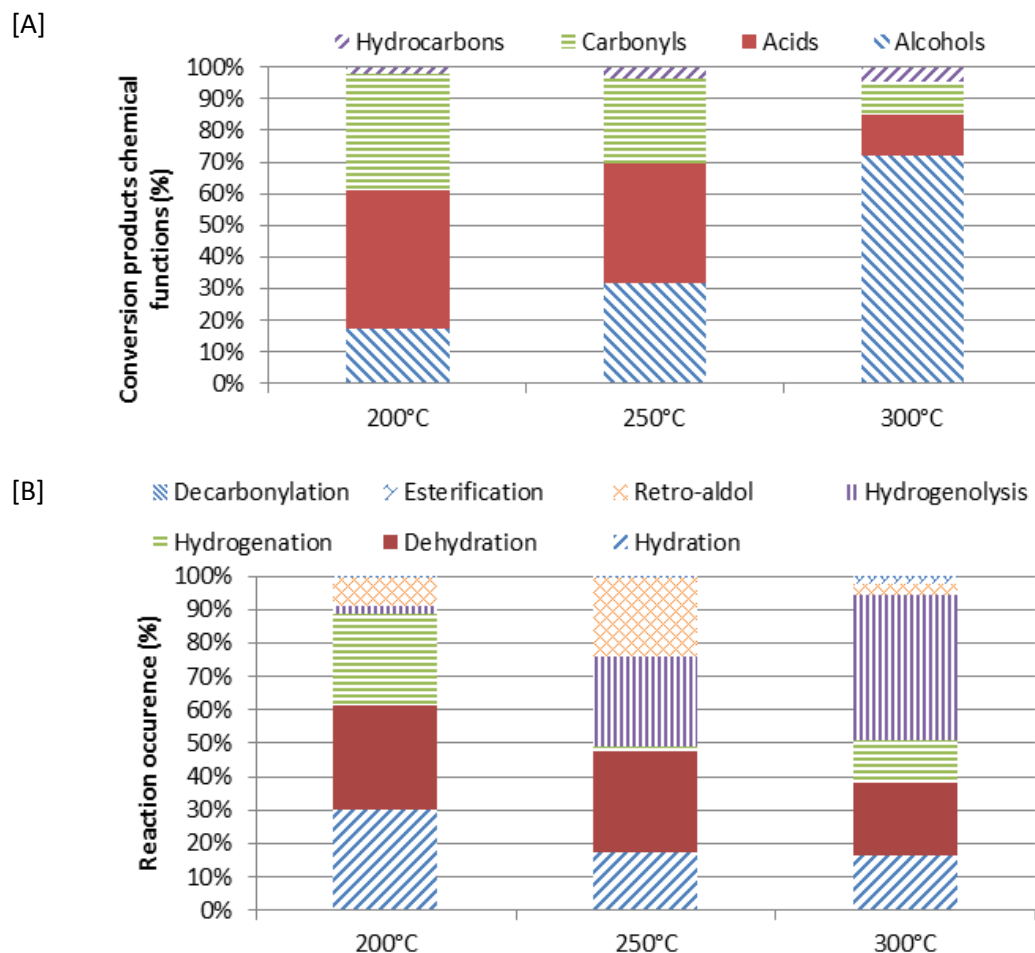


Figure S12: Mixture A quantified products as a function of the temperature (1 h) [A] Chemical functions distribution, [B] Chemical reaction distribution

Figure S13 reports the normalized SEC-UV254 nm analyses of liquid phases from Mixture A as a function of the temperature.

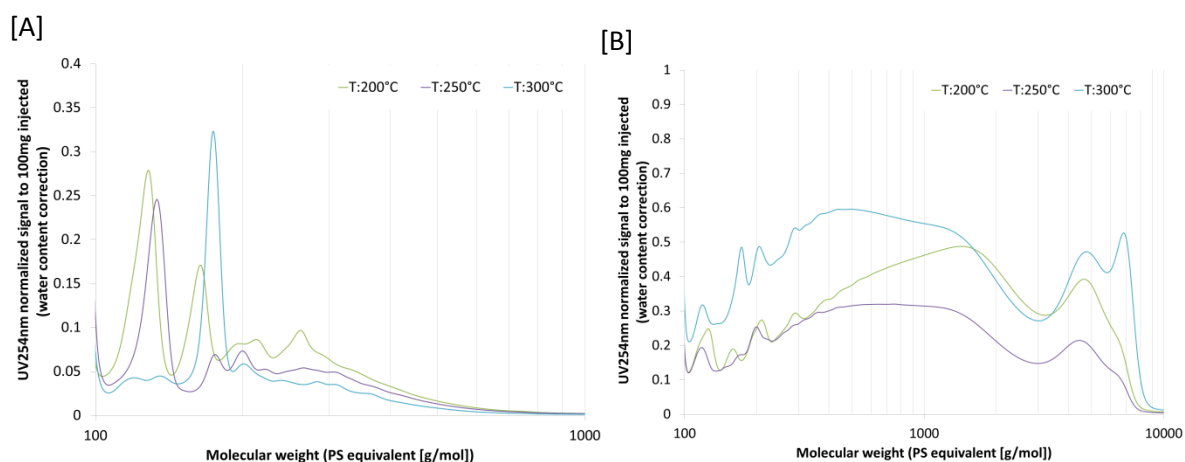


Figure S13 : Normalized SEC-UV254nm analysis of catalytic hydroconverted mixture A as function of reaction temperature (1 h) : [A] Aqueous and [B] Organic phases

Solid from mixtures A hydroconversion at 250 and 300°C were analyzed by ^{13}C NMR. Distribution are reported in Figure S14.

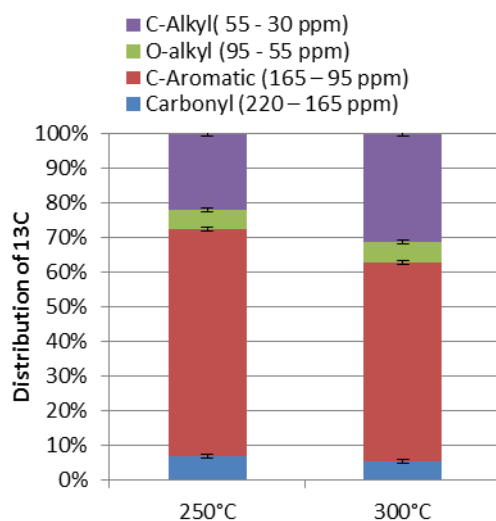
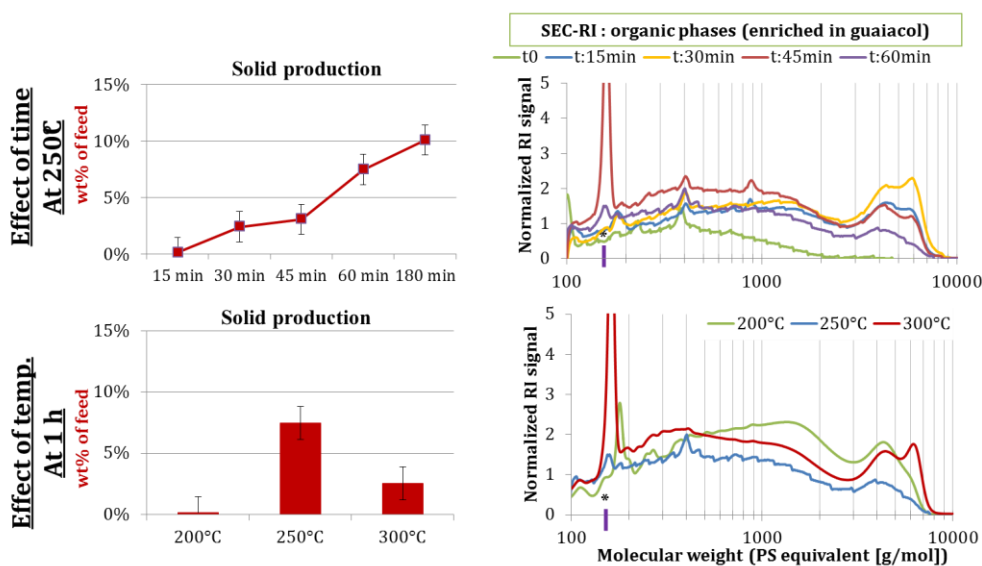


Figure S14 : ^{13}C NMR of Mixture A catalytic hydroconversion solid residues as a function of temperature (1 h)

5-Component mixture : summary of the solid and soluble macromolecule production



Guaiacol interactions with macromolecules

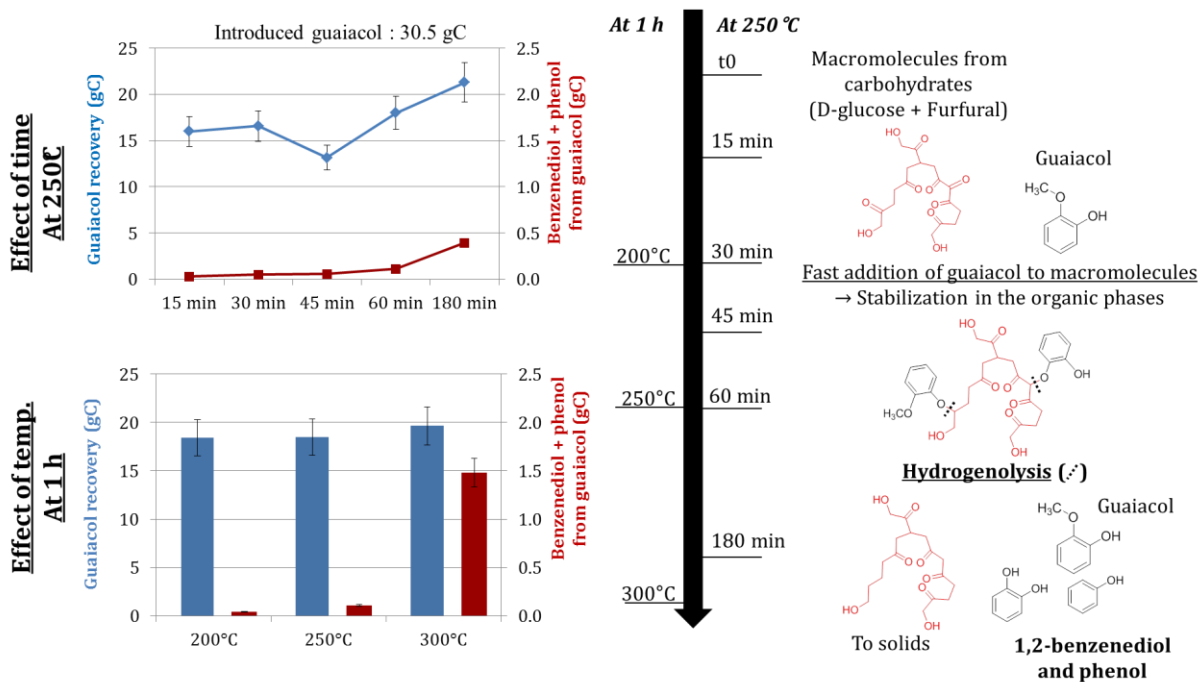


Figure S15 : Summary of the catalytic hydroconversion of the 5-component mixture depending on the reaction time and temperature